MODULAR NONLINEAR FILTER STABILIZATION OF METHODS FOR HIGHER REYNOLDS NUMBERS FLOW

WILLIAM LAYTON*, LEO G. REBHOLZ †, AND CATALIN TRENCHEA ‡

Abstract. Stabilization using filters is intended to model and extract the energy lost to resolved scales due to nonlinearity breaking down resolved scales to unresolved scales. This process is highly nonlinear and yet current models for it use linear filters to select the eddies that will be damped. In this report we consider for the first time nonlinear filters which select eddies for damping (simulating breakdown) based on knowledge of how nonlinearity acts in real flow problems. The particular form of the nonlinear filter allows for easy incorporation of more knowledge into the filter process and its computational complexity is comparable to calculating a linear filter of similar form. We then analyze nonlinear filter based stabilization for the Navier-Stokes equations. We give a precise analysis of the numerical diffusion and error in this process.

1. Introduction.

This report develops a *nonlinear filter* based stabilization to:

adapt model plus numerical dissipation to the localized and intermittent breakdown of eddies by the NSE nonlinearity.

When the resulting smallest persistent and energetically significant scale is significantly larger than the meshwidth, a high Re simulation is over diffused. When the smallest such scale is smaller than the meshwidth, typically nonphysical wiggles are observed and the simulation is under diffused. A successfully tuned model plus numerical method will yield a simulation of a higher Reynolds number flow for which

$$\text{microscale} = \text{filter radius} = \text{(pre-specified) spacial mesh-width.}$$

Nonlinear terms break down eddies into smaller ones until they are small enough for molecular viscosity (in the continuum NSE) or for eddy or numerical dissipation (in the model) to damp them rapidly. This *transfer of energy* (indeed the entire energy cascade), while *modeled* by dissipation terms in simulations, is due to *nonlinearity* in the real flow.

Herein we develop nonlinear filter stabilizations which tune the amount and location of eddy viscosity to the local flow structures and whether the nonlinearity tends to break marginally resolved scales down to smaller scales or let the local structure persist. Indeed, nonlinearity does not break down scales uniformly. Intermittence, nonuniformity, locality and even backscatter are typical features in the energy cascade of high Reynolds number flow problems. We also give a path for further development of models where subsequent improvement (as our understanding of turbulent flows improves) are easy to incorporate into models (with rigorous analytic foundations) and flow simulation codes.

To introduce the ideas, consider the Navier-Stokes equations (NSE) under no slip boundary conditions in a polyhedral domain $\Omega \subset \mathbb{R}^d, (d = 2, 3)$:

$$\begin{aligned} u_t + u \cdot \nabla u - \nu \triangle u + \nabla p = f(x,t). \text{ in } \Omega \times (0,T], \\ \nabla \cdot u = 0 \text{ in } \Omega \times (0,T],\ u = 0 \text{ on } \partial\Omega \times (0,T],\ \text{and}\ \ u(x,0) = u^0(x) \text{ in } \Omega. \end{aligned} \tag{1.1}$$

Given a method for the NSE (e.g., in a legacy code) we consider a method for adapting it to high Reynolds number flows that is modular, uncoupled from the basic method for the NSE and is adapted (as described above) to features of turbulence. To fix ideas and focus on the effects of the added nonlinear filtering step we base our analysis on the implicit method. Suppressing the spacial discretization, we analyze herein: given $u^n \simeq u(t^n)$, compute u^{n+1} by

*Department of Mathematics, University of Pittsburgh, Pittsburgh, PA, 15260, USA. email: wjl@pitt.edu. Partially supported by the NSF under grant DMS-0810385.

†Department of Mathematical Sciences, Clemson University, Clemson SC 29634, USA. email: rebholz@clemson.edu. Partially supported by the NSF under grant DMS-0914478.

‡Department of Mathematics, University of Pittsburgh, Pittsburgh, PA, 15260, USA. email: trenchea@pitt.edu.

ALGORITHM 1.1.

$$\textit{\textbf{Step 1:}}\quad \frac{w^{n+1}-u^n}{\triangle t} + w^{n+1}\cdot\nabla w^{n+1} - \nu\triangle w^{n+1} + \nabla p^{n+1} = f^{\,n+1} \tag{1.2}$$

$$\textit{and } \nabla\cdot w^{n+1} = 0, \tag{1.3}$$

$$\textit{\textbf{Step 2:}}\quad \textit{Nonlinear filter:}\quad w^{n+1} \to \overline{w^{n+1}}, \tag{1.4}$$

$$\textit{\textbf{Step 3:}}\quad \textit{Relax:}\quad u^{n+1} := (1-\chi)w^{n+1} + \chi\overline{w^{n+1}}. \tag{1.5}$$

The essential new ingredient herein is the use of nonlinear filters for Step 2. We define velocity averages $\overline{u}$ so that the fluctuating part $u' := u - \overline{u} \doteq 0$ when the local flow condition is laminar or a structure which persists (not broken down rapidly into smaller structures by the nonlinearity). To specify this nonlinear filter, we select an *indicator function* $a = a(u, \nabla u, \cdots)$ (denoted by $a(u)$) with the properties:

$$0 \le a(u) \le 1 \text{ for any fluid velocity } u(x,t),$$
$$a(u) \simeq 0 \text{ selects regions requiring no local filtering,}$$
$$a(u) \simeq 1 \text{ selects regions requiring } O(\delta) \text{ local filtering.}$$

The *geometric average* of indicator functions is again an indicator function making *increasing the selectivity of indicator functions easy.* Given $a(\cdot)$, the filter radius (denoted δ and related to the meshwidth) and an approximate velocity $w(x,t)$ from Step 1 we define its nonlinearly filtered average $\overline{w}(x,t)$ as the solution, under appropriate boundary conditions, of

$$-\nabla\cdot\left(\delta^2 a(w)\nabla\overline{w}\right) + \nabla\lambda + \overline{w} = w, \text{ and } \nabla\cdot\overline{w} = 0 \text{ in } \Omega. \tag{1.6}$$

Note that when filtering a known velocity, *nonlinear filtering requires solving a linear problem.* Further, with common FEM discretizations of the filter problem and with averaging radius $\delta = O(\triangle x)$ the condition number of the $1,1$ block in the associated mixed type linear system is $O(1)$.

To motivate Steps 2 and 3, let $\chi = 1$ (meaning no relaxation) and rearrange Steps 1 and 2. This gives

$$\frac{u^{n+1}-u^n}{\triangle t} + w^{n+1}\cdot\nabla w^{n+1} - \nu\triangle w^{n+1} + \nabla p^{n+1} + \frac{1}{\triangle t}(w^{n+1} - \overline{w^{n+1}}) = f^{\,n+1} \tag{1.7}$$

which is a time relaxation discretization of the NSE with relaxation coefficient $1/\triangle t$. From (1.6), using $u = \overline{w}$ and $w - \overline{w} = -\delta^2\nabla\cdot(a(w)\nabla u) + \nabla\lambda$ gives

$$\frac{u^{n+1}-u^n}{\triangle t} + w^{n+1}\cdot\nabla w^{n+1} - \nu\triangle w^{n+1} + \nabla\left(p^{n+1} + \lambda^{n+1}\right) - \frac{\delta^2}{\triangle t}\nabla\cdot\left(a(w^{n+1})\nabla u^{n+1}\right) = f^{n+1}.$$

Thus, the effect of the nonlinear filter in Step 2 is to implement a given nonlinear eddy viscosity model via a modular Step 2 uncoupled from whatever method is used to advance in time in Step 1. The artificial viscosity coefficient is $\delta^2/\triangle t$ which can result in low accuracy and large amounts of numerical diffusion depending on the relative scalings of $\triangle t$ and δ. We shall also see that the effect of the relaxation in Step 3 is to reduce the eddy viscosity coefficient to a given desired level.

REMARK 1.2 (Nonlinear Filters). *We have selected the simplest time discretization in Step 1 to focus attention on the effect of the nonlinearity in the filter step. Our results herein extend immediately to the linearly implicit method (with $u^{n+1}\cdot\nabla u^{n+1}$ replaced by $u^n\cdot\nabla u^{n+1}$) and can be extended to the Crank-Nicolson (which is used in the experiments in Section 6) and BDF2 methods for Step 1. At this point the best treatment of the pressure in Steps 2 and 3 is an open problem. We stress that modularity of Steps 2 and 3 is one important aspect of this formulation: a given turbulence model can be implemented in a fluids code by treating the fluids code as a black box solver.*

1.1. Related work. There has been a substantial amount of previous study of *linear* filter based stabilization. Linear filter based stabilization was developed by Boyd [Boyd98] and Fischer and Mullen [FM01], [MF98] and was used by Dunca [D02]. Mathew et al. [MLF03] made the important connection that an uncoupled Step 2 (as above) induces a new implicit time relaxation term into the discretization as in (1.7), see also Section 5.3.3 in Garnier, Adams and Sagaut [GAS09] and Visbal and Rizzetta [VR02]. The connection to (linear) time relaxation links to work of Schochet and Tadmor [ST92], Roseneau [R89], Adams, Kleiser, Leonard and Stolz [AL99], [AS01], [AS02], [SA99], [SAK01a], [SAK01b], [SAK02], Dunca [D02], [D04], [DE04] and [LN07], [LMNR06], [ELN07], [L07b], [CL08]. The relaxation step (Step 3) was introduced by Fischer and Mullen [FM01], [MF98] to keep numerical diffusion from blowing up as $\triangle t \to 0$. Our analysis in the linear case in [ELN10] has shown its importance, confirmed by experiments.

2. Nonlinear Filters. The idea we present is to adapt simpler models through the filter instead of using a simple filter and adapting by a sequence of turbulence models of increasing complexity and fitting parameters. This has the computational advantages of algorithmic modularity and homogeneity as well as the modeling advantages of giving a clear path for increasing model accuracy. Indeed, given a black-box code for laminar incompressible flow, incompressible turbulence can be solved by adding an independent filtering subroutine. Further, once the filtering subroutine is written, further refinement of the turbulence model can be made through function subroutines defining more indicator functions $a_i(\cdot), i = 1, \cdots, M$ whereupon

$$a(u) := \left(\prod_{i=1}^{M} a_i(u) \right)^{1/M} \tag{2.1}$$

Definition 2.1. *Let u be a fluid velocity. By an indicator function $a = a(u, \nabla u. \cdots)$ (and abbreviated as $a(u)$) we shall mean a scalar valued function of $u, \nabla u$ and other flow variables with range $[0, 1]$,*

$$0 \le a(u) \le 1$$

selected with the intent that

$$a(u(x)) \doteq 0 \textit{ for laminar regions or persistent flow structures,}$$
$$a(u(x)) \doteq 1 \textit{ for flow structures which decay rapidly.}$$

Several examples of indicator functions are given in Section 3.

Definition 2.2 (Nonlinear Filter). *Given an indicator function $a(\cdot)$, a fluid velocity u and an averaging radius δ (possibly varying with x), we define the nonlinearly filtered velocity $\overline{u}$ and associated fluctuation $u' := u - \overline{u}$ using the selected indicator function as the solution of*

$$\begin{gathered} -\nabla \cdot (\delta^2 a(u) \nabla \overline{u}) + \overline{u} + \nabla \lambda = u, \textit{ in the flow domain } \Omega, \\ \nabla \cdot \overline{u} = 0 \textit{ , in } \Omega, \textit{ and } \overline{u} = u \textit{ , on } \partial\Omega. \end{gathered} \tag{2.2}$$

Other boundary conditions can be considered. Also the idea can be extended to other local averaging (non-differential) filters. Various regularizations of the filter are possible and may be necessary for practical computations. Note that if $a(u) \equiv 1$ nonlinear filters reduce to the commonly seen linear differential filter, Germano [Ger86] and that

$$\overline{u} \doteq u, \text{ i.e. } u' \doteq 0, \text{ where } a(u) \doteq 0.$$

2.1. Discrete Nonlinear Filters. Filters are computed relative to a given computational mesh. We shall thus define the discrete nonlinear filter to be the finite element approximation to (2.2). We base our analysis on the finite element method (FEM) for the spacial discretization. (The results extend to many other variational methods.)

The $L^2(\Omega)$ norm and inner product will be denoted by $\|\cdot\|$ and $(\cdot, \cdot)$. Likewise, the $L^p(\Omega)$ norms and the Sobolev $W_p^k(\Omega)$ norms are denoted by $\|\cdot\|_{L^p}$ and $\|\cdot\|_{W_p^k}$, respectively. For the semi-norm in $W_p^k(\Omega)$ we use $|\cdot|_{W_p^k}$. H^k is used to represent the Sobolev space $W_2^k(\Omega)$, and $\|\cdot\|_k$ denotes the norm in H^k. The space H^{-k} denotes the dual space of H_0^k. For functions $v(x,t)$ defined on the entire time interval $(0,T)$, we define $(1 \le m < \infty)$

$$\|v\|_{\infty,k} := \operatorname*{ess\,sup}_{[0,T]} \|v(t,\cdot)\|_k \,, \text{ and } \|v\|_{m,k} := \left(\int_0^T \|v(t,\cdot)\|_k^m \, dt \right)^{1/m} .$$

To begin, under no slip boundary conditions we denote the velocity and pressure spaces by

$$X := (H_0^1(\Omega))^d,\ Q := L_0^2(\Omega).$$

We use as the norm on X , $\|v\|_X := \|\nabla v\|_{L^2}$, and denote the dual space of X by $X^\star$,with the norm $\|\cdot\|_\star$. The space of divergence free functions is given by

$$V := \{v \in X :\ (\nabla \cdot v, q) = 0\ \ \forall q \in Q\}\,.$$

We shall denote conforming velocity, pressure finite element spaces based on an edge to edge triangulations of Ω (with maximum triangle diameter h) by

$$X_h \subset X,\ Q_h \subset Q.$$

We shall assume that $X_h,\ Q_h$ satisfy the usual inf-sup condition necessary for the stability of the pressure, e.g. [G89]. The discretely divergence free subspace of X_h is

$$V_h = \{v_h \in X_h : (\nabla \cdot v_h, q_h) = 0\ \ \forall q_h \in Q_h\}\,.$$

Taylor-Hood elements (see e.g. [BS94, G89]) are one common example of such a choice for (X_h, Q_h), and are also the elements we use in our numerical experiments.

Since the indicator function can be very small on some sub-regions we include grad-div stabilization (see, e.g., [LMNOR09] and references therein).

Definition 2.3 (Discrete Nonlinear Filter). *Assume that $X_h,\ Q_h$ satisfies the discrete inf-sup condition. Given an indicator function $a(\cdot)$, a fluid velocity $u \in V$, an averaging radius δ (possibly varying with x), and $\gamma > 0$ an $O(1)$ parameter, we define the nonlinearly filtered velocity $\overline{u}^h$ using the selected indicator function as the solution of: $(\overline{u}^h, \lambda_h) \in X_h \times Q_h$ is the unique solution of*

$$(\delta^2 a(u)\nabla\overline{u}^h, \nabla v_h) + \gamma(\nabla\cdot\overline{u}^h, \nabla\cdot v_h) + (\overline{u}^h, v_h) - (\lambda_h, \nabla\cdot v_h) = (u, v_h)\ \ \forall v_h \in X_h\,, \tag{2.3}$$

$$(\nabla\cdot\overline{u}^h, q) = 0\ \ \forall q \in Q_h. \tag{2.4}$$

This is equivalent to: For $u \in V$, $\delta > 0$ given and $\gamma > 0$ an $O(1)$ parameter, the averaged velocity $\overline{u}^h \in V_h$ is the unique solution of

$$(\delta^2 a(u)\nabla\overline{u}^h, \nabla v_h) + \gamma(\nabla\cdot\overline{u}^h, \nabla\cdot v_h) + (\overline{u}^h, v_h) = (u, v_h)\ \ \forall v_h \in V_h\,. \tag{2.5}$$

Proposition 2.4. *Assume that $X_h,\ Q_h$ satisfies the discrete inf-sup condition. Consider the discrete nonlinear filter $\overline{u}^h$ given by (2.3). $\overline{u}^h$ exists uniquely and satisfies*

$$\gamma||\nabla\cdot\overline{u}^h||^2 + \int_\Omega \delta^2 a(u)|\nabla\overline{u}^h|^2 dx + \frac{1}{2}||\overline{u}^h||^2 + \frac{1}{2}||u - \overline{u}^h||^2 = \frac{1}{2}||u||^2,$$

$$\gamma||\nabla\cdot\overline{u}^h||^2 + \int_\Omega \delta^2 a(u)|\nabla\overline{u}^h|^2 dx + \frac{1}{2}||\overline{u}^h||^2 \le \frac{1}{2}||u||^2.$$

Proof. For the á priori bound, set $v_h = \overline{u}^h$ in (2.5). Using the polarization identity on the RHS gives

$$\gamma||\nabla\cdot\overline{u}^h||^2 + \int_\Omega \delta^2 a(u)|\nabla\overline{u}^h|^2 dx + ||\overline{u}^h||^2 = (u, v_h) =$$
$$= \frac{1}{2}\left[||u||^2 + ||\overline{u}^h||^2 - ||u - \overline{u}^h||^2\right],$$

from which the result follows. For existence, note that for fixed u,

$$v, w \to (\delta^2 a(u)\nabla v, \nabla w) + \gamma(\nabla\cdot v, \nabla\cdot w) + (v, w)$$

is a continuous and coercive (possibly non-uniformly in h) bilinear form on the finite dimensional space V^h. Thus $\overline{u}^h$ exists uniquely. ∎

We now consider the error in nonlinear filtering of smooth functions.

THEOREM 2.5 (Error in Nonlinear Filters). *Let X_h, Q_h satisfy the inf-sup condition and $u \in V$. Consider the discrete nonlinear filter $\overline{u}^h$ given by (2.3). We have*

$$\gamma||\nabla \cdot \overline{u}^h||^2 + \int_\Omega \delta^2 a(u)|\nabla(u - \overline{u}^h)|^2 dx + ||u - \overline{u}^h||^2$$
$$\leq C \inf_{\widetilde{u} \in V_h} \left\{ \gamma||\nabla \cdot (u - \widetilde{u})||^2 + \int_\Omega \delta^2 a(u)|\nabla(u - \widetilde{u})|^2 dx + ||u - \widetilde{u}||^2 \right\} + C\delta^4_{\max}||\nabla \cdot (a(u)\nabla u)||^2.$$

Proof. We first derive the error equation. Subtracting both sides of (2.3) from $u - \nabla \cdot (\delta^2 a(u)\nabla u)$ and denoting $e = u - \overline{u}^h$ gives

$$(\delta^2 a(u)\nabla e, \nabla v_h) - \gamma(\nabla \cdot \overline{u}^h, \nabla \cdot v_h) + (e, v_h) + (\lambda_h, \nabla \cdot v_h) = -(\nabla \cdot (\delta^2 a(u)\nabla u), v_h)\ , \forall v_h \in X_h. \quad (2.6)$$

For $v_h \in V_h$ the pressure term is zero and this simplifies (2.6) to

$$(\delta^2 a(u)\nabla e, \nabla v_h) - \gamma(\nabla \cdot \overline{u}^h, \nabla \cdot v_h) + (e, v_h) = -(\nabla \cdot (\delta^2 a(u)\nabla u), v_h)\ , \forall v_h \in V_h\,. \quad (2.7)$$

Split the error as $e = u - \overline{u}^h = \eta - \phi_h$ where $\eta = u - \widetilde{u}$, $\phi_h = \overline{u}^h - \widetilde{u}$ for a fixed but arbitrary $\widetilde{u} \in V_h$. Rearranging the error equation and setting $v_h = \phi_h$ gives

$$\gamma||\nabla \cdot \phi_h||^2 + \int_\Omega \delta^2 a(u)|\nabla \phi_h|^2 dx + ||\phi_h||^2$$
$$= (\delta^2 a(u)\nabla \eta, \nabla \phi_h) + \gamma(\nabla \cdot \eta, \nabla \cdot \phi_h) + (\eta, \phi_h) + (\nabla \cdot (\delta^2 a(u)\nabla u), \phi_h)$$
$$\leq \gamma||\nabla \cdot (u - \widetilde{u})||^2 + \int_\Omega \frac{\delta^2}{2}\left[a(u)|\nabla \eta|^2 + a(u)|\nabla \phi_h|^2\right] dx + \frac{1}{2}\left[||\eta||^2 + ||\phi_h||^2\right] +$$
$$+ C\delta^4_{\max}||\nabla \cdot (a(u)\nabla u)||^2 + \frac{1}{4}||\phi_h||^2.$$

The triangle inequality plus the observation that $||\nabla \cdot (u - \overline{u}^h)|| = ||\nabla \cdot \overline{u}^h||$ completes the proof. □

3. Three Examples of Indicator Functions and Nonlinear Filters.

The most mathematically convenient indicator function, recovering variants of the Smagorinsky model, is $a(u) = |\nabla u|$ (suitably normalized [BIR09]) due to its strong monotonicity property. However, it is well known that the Smagorinsky model is not sufficiently selective, [S01]. Indeed, this choice incorrectly selects laminar shear flow (where $|\nabla u|$ is constant but large) as sites of large turbulent fluctuations. Insight into construction of indicator functions of increased accuracy can be obtained from theories of intermittence and eduction. In some respects, theories of intermittence are complementary to theories of eduction of coherent and persistent flow structures. Both therefore have insights that can be used to sharpen the indicator function used in nonlinear filtering. In this section we show how several can be adapted to give indicator functions. Since the geometric average of indicator functions is a more selective indicator function, examples are not isolated but give a path for successive improvements.

3.1. The Q criterion.

Let the deformation and spin tensors be denoted, respectively

$$\nabla^s u := \frac{1}{2}\left(\nabla u + \nabla u^{tr}\right) \quad \text{and} \quad \nabla^{ss} u := \frac{1}{2}\left(\nabla u - \nabla u^{tr}\right).$$

The most popular method for eduction of coherent vortices is the Q criterion of Hunt, Wray and Moin [HWM88] which marks as a persistent and coherent vortex those regions where

$$Q(u, u) := \frac{1}{2}\left(\nabla^{ss} u : \nabla^{ss} u - \nabla^s u : \nabla^s u\right) > 0.$$

Thus $Q > 0$ occurs in those regions where spin (local rigid body rotation) dominates deformation. It is known to be a necessary condition (in 3d) and both necessary and sufficient (in 2d) for slower than exponential local separation of trajectories.

An indicator function is obtained by rescaling $Q(u,u)$ so that the condition $Q(u,u) > 0$ implies $a(u) \simeq 0$ so that $u \simeq \overline{u}$ and $u' \simeq 0$. There are many plausible ways to do this. We shall test the following.

DEFINITION 3.1. *The Q-criterion based indicator function is given by*

$$a_Q(u) := \frac{1}{2} - \frac{1}{\pi}\arctan\left(\delta^{-1}\frac{Q(u,u)}{Q(u,u)+\delta^2}\right).$$

3.2. Vreman's eddy viscosity. Perhaps the most advanced and elegant eddy viscosity model has recently been proposed by Vreman [V04]. In a very deep construction, using only the gradient tensor he constructs an eddy viscosity coefficient formula that vanishes identically for 320 types of flow structures that are known to be coherent (non turbulent). Define

$$|\nabla w|_F^2 = \sum_{i,j=1,2,3}(\frac{\partial u_j}{\partial x_i})^2, \beta_{ij} := \sum_{m=1,2,3}\frac{\partial u_i}{\partial x_m}\frac{\partial u_j}{\partial x_m}, \text{ and}$$
$$B(u)\ : = \beta_{11}\beta_{22} - \beta_{12}^2 + \beta_{11}\beta_{33} - \beta_{13}^2 + \beta_{22}\beta_{33} - \beta_{23}^2.$$

In $2d$, $B(u)$ simplifies to

$$B(u) = \left[\left(\frac{\partial u_1}{\partial x_1}\right)^2 + \left(\frac{\partial u_1}{\partial x_2}\right)^2\right]\left[\left(\frac{\partial u_2}{\partial x_1}\right)^2 + \left(\frac{\partial u_2}{\partial x_2}\right)^2\right] - \left[\frac{\partial u_1}{\partial x_1}\frac{\partial u_2}{\partial x_1} + \frac{\partial u_1}{\partial x_2}\frac{\partial u_2}{\partial x_2}\right]^2.$$

With C a positive tuning constant, it is given as follows

$$\text{Vreman's eddy viscosity coefficient} = C\delta^2\left\{\begin{array}{c}\sqrt{\frac{B(u)}{|\nabla u|_F^4}}, \text{ if } |\nabla w|_F \neq 0\\ 0, \text{ if } |\nabla w|_F = 0.\end{array}\right\}$$

Since $0 \leq B(u)/|\nabla u|_F^4 \leq 1$ we take as indicator function the following.

DEFINITION 3.2. *The Vreman based indicator function is*

$$a_V(u) = \sqrt{\frac{B(u)}{|\nabla u|_F^4}}.$$

3.3. Relative helicity density. The relative helicity density is the helicity density scaled by the magnitude of velocity and vorticity.

DEFINITION 3.3. *Let $\omega = \nabla \times u$. The helicity $H(t)$, helicity density $HD(x,t)$ and relative helicity density $RH(x,t)$ are given respectively as follows*

$$H(t) := \frac{1}{|\Omega|}\int_\Omega u\cdot\omega dx, HD(x,t) := \frac{1}{|\Omega|}u(x,t)\cdot\omega(x,t), \text{ and } RH(x,t) := \frac{u(x,t)\cdot\omega(x,t)}{|u(x,t)||\omega(x,t)|}.$$

If the NSE nonlinearity is in rotational form, the helicity, $u\cdot\omega$, and the NSE nonlinearity, $u\times\omega$, are related by

$$\frac{\text{Helicity}^2 + |\text{ NSE nonlinearity}|^2}{|u|^2|\omega|^2} = 1.$$

Thus (local) high helicity suppresses (local) turbulent dissipation caused by breakdown of eddies into smaller ones by the NSE nonlinearity. For example, Lilly [Lilly86] notes that storm cells (with low helicity) break down rapidly due to nonlinear interactions while rotating "supercell" thunderstorms (with high helicity) maintain their structure over much longer time scales. Different rates of eddy breakdown due to (local) high or low helicity has even been taken to explain intermittence, Levich and Tsoniber [LT83], [LT83b], [TL83], Betchov [B61].

Thus we develop an indicator function by adjusting relative helicity density so the values near one imply $a(u) \simeq 0$ so that $u \simeq \overline{u}$. Among the many possibly ways to do this, we propose the following.

DEFINITION 3.4. *The relative helicity based indicator function is given by*

$$a_H(u) := 1 - \left| \frac{u(x,t) \cdot \omega(x,t)}{|u(x,t)||\omega(x,t)| + \delta^2} \right|.$$

4. Nonlinear Filter Based Stabilization. The fundamental problem of both eddy viscosity models and filter based stabilization is that, if not carefully done, they reduce accuracy by introducing large amounts of numerical or model diffusion. To identify this mechanism, we suppress the spacial discretization in this (short preliminary) section. We consider the Navier-Stokes equations (NSE) in a polyhedral domain $\Omega \subset \mathbb{R}^d, (d = 2 \text{ or } 3)$

$$\begin{gathered} u_t + u \cdot \nabla u - \nu \triangle u + \nabla p = f(x,t) \;\;, \text{ in } \Omega,\; t > 0, \\ \nabla \cdot u = 0, \;\; \text{in } \Omega,\; t > 0, \;\; \text{and} \;\; u = 0 \text{ on } \partial\Omega \text{ for } t > 0, \\ u(x,0) = u^0(x), \text{ in } \Omega. \end{gathered} \tag{4.1}$$

We shall assume that the solution to the NSE that is approximated is a strong solution and in particular satisfies, recalling that $X = (H_0^1(\Omega))^d$,

$$\begin{aligned} & u \in L^2(0,T;X) \cap L^\infty(0,T;L^2(\Omega)) \cap L^4(0,T;X), \\ & p \in L^2(0,T;Q), \;\; u_t \in L^2(0,T;X^*)\,. \end{aligned} \tag{4.2}$$

ALGORITHM 4.1. *Pick $\chi \in [0,1]$ and $\triangle t > 0$.*
Step 1: Given u^n, p^n find w^{n+1} satisfying

$$\begin{gathered} \frac{w^{n+1} - u^n}{\triangle t} + w^{n+1} \cdot \nabla w^{n+1} - \nu \triangle w^{n+1} + \nabla p^{n+1} = f^{\,n+1} \\ \nabla \cdot w^{n+1} = 0 \;\; \text{and} \;\; w^{n+1} = 0 \;, \text{ on } \partial\Omega. \end{gathered} \tag{4.3}$$

Step 2: Filter: Compute $\overline{w^{n+1}}$ by solving (a discrete version) of

$$\begin{gathered} -\delta^2 \nabla \cdot \left(a(w^{n+1}) \nabla \overline{w^{n+1}} \right) + \overline{w^{n+1}} + \nabla \lambda = w^{n+1}, \\ \nabla \cdot \overline{w^{n+1}} = 0, \quad \text{and} \quad \overline{w^{n+1}} = 0 \;, \text{ on } \partial\Omega. \end{gathered}$$

Step 3: Relax:

$$u^{n+1} := (1-\chi) w^{n+1} + \chi \overline{w^{n+1}}.$$

To understand the effect of Steps 2 and 3 on the velocity approximation, the numerical diffusion introduced by Step 2 is quantified.

LEMMA 4.2. *Suppose $0 \le a(w) \le 1$. Consider Algorithm 4.1, Step 2 and let $w, \nabla w \in L^2(\Omega)$ with $w = 0$ on $\partial\Omega$. We have*

$$||\overline{w}|| < ||w|| \text{ unless } a(w) \equiv 0 \text{ and thus } \overline{w} = w; \tag{4.4}$$

specifically

$$||\overline{w} - w||^2 + \int_\Omega 2\delta^2 a(w) |\nabla \overline{w}|^2 dx + ||\overline{w}||^2 = ||w||^2.$$

Further, unless $\overline{w} = 0$,

$$(w, \overline{w}) > 0, \tag{4.5}$$

and, unless $\overline{w} = w$,

$$(w - \overline{w}, w) > 0. \tag{4.6}$$

Finally, in all cases, $(w - \overline{w}, \overline{w}) \geq 0$.

Proof. Take the inner product of the equation $-\delta^2 \nabla \cdot (a(w)\nabla\overline{w}) + \overline{w} + \nabla\lambda = w$ with $\overline{w}$ and the inner product of $\nabla \cdot \overline{w^{n+1}} = 0$ with λ and add. Applying the polarization identity to the RHS gives

$$\int_\Omega \delta^2 a(w)|\nabla\overline{w}|^2 + |\overline{w}|^2 dx = (w, \overline{w}) = \frac{1}{2}||\overline{w}||^2 + \frac{1}{2}||w||^2 - \frac{1}{2}||\overline{w} - w||^2,$$

proving the first claim and the second claim. For the third claim consider $(w - \overline{w}, w)$. By the polarization identity we have

$$\begin{aligned}(w - \overline{w}, w) &= ||w||^2 - \frac{1}{2}\left[||w||^2 + ||\overline{w}||^2 - ||w - \overline{w}||^2\right] \\ &= \frac{1}{2}\left[||w||^2 - ||\overline{w}||^2 + ||w - \overline{w}||^2\right] > 0\end{aligned}$$

since $||w|| > ||\overline{w}||$. Finally consider $(w - \overline{ww})$. Since $w - \overline{w} = -\delta^2\nabla \cdot (a(w)\nabla\overline{w}) + \nabla\lambda$ and $\nabla \cdot \overline{w} = 0$ we have

$$(w - \overline{w}, \overline{w}) = \left(-\delta^2\nabla \cdot (a(w)\nabla\overline{w}), \overline{w}\right) = \int_\Omega \delta^2 a(w)|\nabla\overline{w}|^2 dx \geq 0,$$

completing the proof. ▯

For linear filtering Stanculescu [S07] (see also Manica and Kaya-Merdan [MKM06]) derived three minimal conditions on the filter operator for it to be useful in deconvolution closure models of turbulence. In the case of nonlinear filtering, these are exactly the three conditions (4.4), (4.5), (4.6) proven above.

Theorem 4.3. *Consider Algorithm 4.1. Let* $f = 0$ *and suppose the steps* u^n, w^n, p^n *in Algorithm 4.1 are well defined and sufficiently smooth. Let* $u = (1 - \chi)w + \chi\overline{w}$*. Then*

$$||w^{n+1}||^2 - ||u^{n+1}||^2 = \chi(2 - \chi)\left(w^{n+1} - \overline{w^{n+1}}, w^{n+1}\right) + \chi^2\left(w^{n+1} - \overline{w^{n+1}}, \overline{w^{n+1}}\right). \tag{4.7}$$

An approximate solution given by Algorithm 1.1 satisfies, for any $l > 0$,

$$\begin{aligned}&\frac{1}{2}||u^l||^2 + +\triangle t\sum_{n=0}^{l-1}\left\{\frac{\triangle t}{2}||\frac{w^{n+1} - u^n}{\triangle t}||^2 + \nu||\nabla w^{n+1}||^2\right\} \\ &+\triangle t\sum_{n=0}^{l-1}\left\{\frac{\chi}{\triangle t}\frac{2 - \chi}{2}\left(w^{n+1} - \overline{w^{n+1}}, w^{n+1}\right) + \frac{\chi}{\triangle t}\frac{\chi}{2}\left(w^{n+1} - \overline{w^{n+1}}, \overline{w^{n+1}}\right)\right\} = \frac{1}{2}||u^0||^2.\end{aligned}$$

For $0 \leq \chi \leq 2$ *the following term is non-negative:*

$$\frac{\chi}{\triangle t}\frac{2 - \chi}{2}\left(w^{n+1} - \overline{w^{n+1}}, w^{n+1}\right) + \frac{\chi}{\triangle t}\frac{\chi}{2}\left(w^{n+1} - \overline{w^{n+1}}, \overline{w^{n+1}}\right) \geq 0. \tag{4.8}$$

Proof. Take the L^2 inner product of Step 1 with w^{n+1} and $\nabla \cdot w^{n+1} = 0$ with p^{n+1} and add. Use skew symmetry of the nonlinear terms and the polarization identity to the term $\left(u^n, w^{n+1}\right)$ and rearrange the result. This gives

$$\frac{1}{\triangle t}\left(||u^{n+1}||^2 - ||u^n||^2\right) + \frac{1}{\triangle t}||u^n - w^{n+1}||^2 + 2\nu||\nabla w^{n+1}||^2 + \frac{1}{\triangle t}\left[||w^{n+1}||^2 - ||u^{n+1}||^2\right] = 0. \tag{4.9}$$

Suppressing the superscripts $n + 1$, Step 3 can be rearranged to read

$$u + \chi(w - \overline{w}) = w$$

Take the L^2 inner product with w. This gives

$$(u, w) + \chi (w - \overline{w}, w) = ||w||^2$$

By the last Lemma, the second term is nonnegative, $\chi (w - \overline{w}, w) \geq 0$. Apply the polarization identity to the first term and multiply by 2. This gives

$$||u||^2 - ||u - w||^2 + 2\chi (w - \overline{w}, w) = ||w||^2.$$

Step 3 can also be rearranged to read

$$u - w = -\chi(w - \overline{w}), \quad \text{so} \quad ||u - w||^2 = \chi^2 ||w - \overline{w}||^2 = \chi^2 (w - \overline{w}, w - \overline{w}).$$

Thus,

$$\begin{aligned} ||w||^2 &= ||u||^2 - \chi^2 (w - \overline{w}, w - \overline{w}) + 2\chi (w - \overline{w}, w) \\ &= ||u||^2 + \chi(2 - \chi) (w - \overline{w}, w) + \chi^2 (w - \overline{w}, \overline{w}), \end{aligned}$$

which is the first claim. Inserting this with $u = u^{n+1}, w = w^{n+1}$ into (4.9) gives

$$\begin{aligned} &\frac{1}{\triangle t} \left(||u^{n+1}||^2 - ||u^n||^2 \right) + \frac{1}{\triangle t} ||u^n - w^{n+1}||^2 + 2\nu ||\nabla w^{n+1}||^2 + \\ &+ \frac{\chi}{\triangle t} \left[\frac{2 - \chi}{2} \left(w^{n+1} - \overline{w^{n+1}}, w^{n+1} \right) + \frac{\chi}{2} \left(w^{n+1} - \overline{w^{n+1}}, \overline{w^{n+1}} \right) \right] = 0. \end{aligned}$$

Summing gives the energy estimate. The last claim that the indicated is nonnegative follows from the Lemma 4.2. □

This theorem identifies the viscous dissipation and numerical dissipation in Step 1 as

$$\begin{aligned} \text{Viscous Dissipation} &= \nu ||\nabla w^{n+1}||^2, \\ \text{Numerical Dissipation in Step 1} &= \frac{\triangle t}{2} || \frac{w^{n+1} - u^n}{\triangle t} ||^2. \end{aligned}$$

The model / numerical dissipation introduced by Steps 2 and 3 is

$$\frac{\chi}{\triangle t} \left[\frac{2 - \chi}{2} \left(w^{n+1} - \overline{w^{n+1}}, w^{n+1} \right) + \frac{\chi}{2} \left(w^{n+1} - \overline{w^{n+1}}, \overline{w^{n+1}} \right) \right]. \tag{4.10}$$

REMARK 4.4. *The form of the numerical diffusion induced by Algorithm 4.1 suggests the natural scaling (used in our tests in the linear case in [ELN10])*

$$\chi \simeq O(\triangle t).$$

With this scaling the second and third terms in the numerical dissipation are higher order; the numerical dissipation is dominated by the first term $(\chi / \triangle t) (w - \overline{w}, w)$.

5. Error Analysis of the fully discrete approximation. In the last section we have suppressed in the stability analysis the spacial discretization. In the error analysis the coupling between the various errors in Algorithm 5.1 below plays a key role so the spacial discretization is no longer secondary. We base our analysis on the finite element method (FEM) for the spacial discretization (and believe that the results extend to many other variational methods).

The notation for conforming velocity-pressure FEM spaces $X_h \subset X$, $Q_h \subset Q$ is defined above. We shall always assume that X_h, Q_h satisfy the usual inf-sup condition (see e.g., [G89, BS94]) necessary for the stability of the pressure. Recall that the discretely divergence free subspace of X_h is

$$V_h = \{ v_h \in X_h : (\nabla \cdot v_h, q_h) = 0 \ \ \forall q_h \in Q_h \}.$$

Define the usual explicitly skew symmetrized trilinear form

$$b^*(u,v,w) := \frac{1}{2}(u\cdot\nabla v, w) - \frac{1}{2}(u\cdot\nabla w, v).$$

We analyze the FEM in space, implicit method in time with nonlinear filtering and relaxation step.

ALGORITHM 5.1. *[Evolve, Nonlinear Filter then Relax]*

Step 1: Evolve: Given u_h^n *find* $w_h^{n+1}\in X_h, p_h^{n+1}\in Q_h$ *satisfying*

$$\begin{aligned}(\frac{w_h^{n+1}-u_h^n}{\triangle t}, v_h) + b^*(w_h^{n+1}, w_h^{n+1}, v_h) + \nu(\nabla w_h^{n+1}, \nabla v_h) - (p_h^{n+1}, \nabla\cdot v_h)&\\ = (f^{n+1}, v_h),\ \textit{for all } v_h\in X_h,&\\ (\nabla\cdot w_h^{n+1}, q_h) = 0,\ \textit{for all } q_h\in Q_h.&\end{aligned} \tag{5.1}$$

Step 2: Filter w_h^{n+1} *to give* $(\overline{w}^h, \lambda_h)\in X_h\times Q_h$ *as the unique solution of*

$$\begin{aligned}(\delta^2 a(w_h^{n+1})\nabla\overline{w}^h, \nabla v_h) + \gamma(\nabla\cdot\overline{w}^h, \nabla\cdot v_h) + (\overline{w}^h, v_h) - (\lambda_h, \nabla\cdot v_h) = (w_h^{n+1}, v_h)\quad \forall v_h\in X_h\,,\\ (\nabla\cdot\overline{w}^h, q) = 0\quad \forall q\in Q_h.\end{aligned} \tag{5.2}$$

Step 3: Relax: $\quad u_h^{n+1} := (1-\chi)w^{n+1} + \chi\overline{w}^h.$

The temporal consistency error (in one step) is *Temporal Consistency Error* $= O(\triangle t^2 + \chi||w_h^{n+1} - \overline{w_h^{n+1}}^h||)$. The *forecasted* global error in Algorithm (5.1) is thus

$$\text{Global Error} = O(\triangle t + \frac{\chi\delta^2}{\triangle t} + \text{Spacial Error}).$$

We turn to stability.

LEMMA 5.2. *Assume that* $X_h,\ Q_h$ *satisfies the discrete inf-sup condition. Consider the discrete nonlinear filter* $\overline{w}^h$ *given by (2.3).* $\overline{w}^h$ *exists uniquely and satisfies*

$$\gamma||\nabla\cdot\overline{w}^h||^2 + \int_\Omega \delta^2 a(w)|\nabla\overline{w}^h|^2 dx + \frac{1}{2}||\overline{w}^h||^2 + ||w-\overline{w}^h||^2 = \frac{1}{2}||w||^2,\ \textit{thus}\ \ ||\overline{w}^h|| \le ||w||\,.$$

Let $u_h = (1-\chi)w_h + \chi\overline{w_h}^h$. *Then*

$$||w_h||^2 - ||u_h||^2 = \chi(2-\chi)(w_h - \overline{w_h}^h, w_h) + \chi^2(w_h - \overline{w_h}^h, \overline{w_h}^h),\ \textit{and} \tag{5.3}$$

$$||w_h||^2 - ||u_h||^2 = -||u_h - w_h||^2 + 2\chi(w_h - \overline{w_h}^h, w_h)\,. \tag{5.4}$$

If $0\le\chi\le 1$ *then*

$$||u_h|| \le ||w_h||\,. \tag{5.5}$$

Proof. The proof of the first two bounds is the same as the continuous space case in Lemma 4.2. The proof of third equality is also the same as the continuous case in Theorem 4.3. For the fourth estimate, take the inner product of $u_h = (1-\chi)w_h + \chi\overline{w_h}^h$ with w_h. This gives

$$(u_h, w_h) = (1-\chi)(w_h, w_h) + \chi(\overline{w_h}^h, w_h) = ||w_h||^2 - \chi(w - \overline{w_h}^h, w_h).$$

Applying the polarization identity to the LHS we obtain

$$\frac{1}{2}||w_h||^2 + \frac{1}{2}||u_h||^2 - \frac{1}{2}||u_h - w_h||^2 = (u_h, w_h) = ||w_h||^2 - \chi(w_h - \overline{w_h}^h, w_h).$$

from which (5.4) follows. For (5.5), note that since $||\overline{w_h}^h|| \le ||w_h||$ and $0\le\chi\le 1$,

$$||u_h|| \le (1-\chi)||w_h|| + \chi||\overline{w_h}^h|| \le ((1-\chi)+\chi)\,||w_h|| \le ||w_h||.$$

□

Next we prove an energy equality, unconditional stability and give the precise formula for the numerical dissipation in the algorithm. The energy bound also proves computability of the procedure.

PROPOSITION 5.3. *[Stability] Suppose $0 \leq \chi \leq 1$. Algorithm 5.1 satisfies the energy equality:*

$$\frac{1}{2}||u_h^l||^2 + \triangle t \sum_{n=0}^{l-1} \left\{ \frac{\triangle t}{2} || \frac{w_h^{n+1} - u_h^n}{\triangle t} ||^2 + \nu ||\nabla w_h^{n+1}||^2 \right\} +$$
$$\triangle t \sum_{n=0}^{l-1} \frac{\chi}{\triangle t} \left\{ \frac{2-\chi}{2} \left(w_h^{n+1} - \overline{w_h^{n+1}}^h, w_h^{n+1} \right) + \frac{\chi}{2} \left(w_h^{n+1} - \overline{w_h^{n+1}}^h, \overline{w_h^{n+1}}^h \right) \right\} =$$
$$= \frac{1}{2}||u_h^0||^2 + \triangle t \sum_{n=0}^{l-1} (f^{n+1}, w_h^{n+1}), \ \ \textit{for any } l > 0,$$

and the stability bound:

$$\frac{1}{2}||u_h^l||^2 + \triangle t \sum_{n=0}^{l-1} \left[\frac{\triangle t}{2} || \frac{w_h^{n+1} - u_h^n}{\triangle t} ||^2 + \frac{\nu}{2} ||\nabla w_h^{n+1}||^2 \right]$$
$$+ \triangle t \sum_{n=0}^{l-1} \frac{\chi}{\triangle t} \left[\frac{2-\chi}{2} \left(w_h^{n+1} - \overline{w_h^{n+1}}^h, w_h^{n+1} \right) + \frac{\chi}{2} \left(w_h^{n+1} - \overline{w_h^{n+1}}^h, \overline{w_h^{n+1}}^h \right) \right] =$$
$$\leq \frac{1}{2}||u_h^0||^2 + \frac{\triangle t}{2\nu} \sum_{n=0}^{l-1} ||f^{n+1}||_*^2, \ \ \textit{for any } l > 0.$$

Further, under the discrete inf-sup condition w_h^n, $\overline{w_h^n}^h$, u_h^n, p_h^n, exist at each time step.

Proof. The energy equality follows exactly as in Proposition 5.4. Using the Cauchy-Schwarz-Young inequality on the right hand side, subsuming one term into the LHS and summing over the index n, proves the global stability estimate. Existence follows from the á priori bound, the discrete inf-sup condition and a fixed point argument in a standard way. □

The viscous dissipation, the numerical dissipation induced by the backward Euler time discretization in Step 1 in Algorithm 5.1 and the model / numerical dissipation induced by steps 2 and 3 are

$$\text{Viscous dissipation} \ = \nu ||\nabla w_h^{n+1}||^2,$$
$$\text{Numerical dissipation from Step 1} \ = \frac{\triangle t}{2} || \frac{w_h^{n+1} - u_h^n}{\triangle t} ||^2,$$
$$\text{Model / Numerical Dissipation from Steps 2 and 3} =$$
$$= \frac{\chi}{\triangle t} \left[\frac{2-\chi}{2} \left(w_h^{n+1} - \overline{w_h^{n+1}}^h, w_h^{n+1} \right) + \frac{\chi}{2} \left(w_h^{n+1} - \overline{w_h^{n+1}}^h, \overline{w_h^{n+1}}^h \right) \right] \geq 0.$$

5.1. Error Analysis. Let $t^n = n\Delta t$, $n = 0, 1, 2, \dots, N_T$, $T := N_T \Delta t$, recall $f^n = f(t^n)$ and let $d_t f^n := (f^{n+1} - f^n)/\Delta t$. Introduce the following discrete norms:

$$|||v|||_{\infty,k} := \max_{0 \leq n \leq N_T} \|v^n\|_k, \qquad |||v|||_{m,k} := \left(\Delta t \sum_{n=0}^{N_T} \|v^n\|_k^m \right)^{1/m}.$$

For $W(\Omega)$ a function space, we abbreviate $L^p(0,T;W(\Omega))$ as $L^p(W)$ and analogously for $H^k(W), W_4^2(W)$. In order to establish the optimal asymptotic error estimates for the approximation we need to assume that the true solution is more regular than minimally required to be a strong solution (4.2):

$$u \in L^\infty(W_4^{k+1}) \cap L^\infty(H^{2N+2}) \cap H^1(0,T;H^{k+1}(\Omega)) \cap H^3(L^2) \cap W_4^2(H^1), \tag{5.6}$$
$$p \in L^\infty(H^{s+1}), \text{ and } f \in H^2(L^2). \tag{5.7}$$

In the convergence analysis in the main theorem we shall need a technical extension of the error estimate for nonlinear filters that follows next.

PROPOSITION 5.4. *Let X_h, Q_h satisfy the discrete inf-sup condition and $u \in V$. Let $\widetilde{U} \in V_h$ be fixed but arbitrary and let $\theta := u - \widetilde{U}$. Consider the discrete nonlinear filter $\overline{\theta}^h$ of θ. We have*

$$||\theta - \overline{\theta}^h||^2 \leq 4 \inf_{\widetilde{v} \in V_h} \left\{ 2\gamma ||\nabla \cdot (u - \widetilde{v})||^2 + \delta^2 ||\nabla (u - \widetilde{v})||^2 + ||u - \widetilde{v}||^2 \right\} + 4 \int_\Omega \delta^2 |\nabla (u - \widetilde{U})|^2 dx.$$

Proof. We first derive the error equation. Note that θ satisfies the identity:

$$-\nabla \cdot (\delta^2 a(\theta) \nabla \theta) + \theta = \theta - \nabla \cdot (\delta^2 a(\theta) \nabla \theta), \text{ in } \Omega.$$

Let $e = \theta - \overline{\theta}^h$. Subtraction gives the error equation

$$(\delta^2 a(\theta) \nabla e, \nabla v_h) - \gamma(\nabla \cdot \overline{\theta}^h, \nabla \cdot v_h) + (e, v_h) + (\lambda_h, \nabla \cdot v_h) = -(\nabla \cdot (\delta^2 a(\theta) \nabla \theta), v_h) \ , \forall v_h \in X_h \, .$$

For $v_h \in V_h$ the pressure term is zero and this simplifies to read

$$(\delta^2 a(\theta) \nabla e, \nabla v_h) - \gamma(\nabla \cdot \overline{\theta}^h, \nabla \cdot v_h) + (e, v_h) = -(\nabla \cdot (\delta^2 a(\theta) \nabla \theta), v_h) \ , \forall v_h \in V_h \, .$$

Split the error as $e = \theta - \overline{\theta}^h = \eta - \phi_h$ where $\eta = \theta - \widetilde{v}, \phi_h = \overline{\theta}^h - \widetilde{v}$ for a fixed but arbitrary $\widetilde{v} \in V_h$. We note that since $\widetilde{v} \in V_h$ is fixed but arbitrary and $\widetilde{U} \in V_h$ we can write

$$\eta = \theta - \widetilde{v} = u - \widetilde{U} - \widetilde{v} = u - (\widetilde{U} + \widetilde{v}) = u - \widetilde{\widetilde{v}}$$

by defining $\widetilde{\widetilde{v}} = \widetilde{U} + \widetilde{v}$, another fixed but arbitrary member of V_h (over which an infimum will ultimately be taken).

Rearranging the error equation and setting $v_h = \phi_h$, using $|a(\cdot)| \leq 1$ and

$$\begin{aligned}(\nabla \cdot (\delta^2 a(\theta) \nabla \theta), \phi_h) \ &\leq \frac{1}{2} \int_\Omega \delta^2 a(\theta) |\nabla \phi_h|^2 dx + \frac{1}{2} \int_\Omega \delta^2 a(\theta) |\nabla \theta|^2 dx \\ &\leq \frac{1}{2} \int_\Omega \delta^2 a(\theta) |\nabla \phi_h|^2 dx + \frac{1}{2} \int_\Omega \delta^2 |\nabla (u - \widetilde{U})|^2 dx\end{aligned}$$

gives

$$\gamma ||\nabla \cdot \phi_h||^2 + \frac{1}{4} ||\phi_h||^2 \leq \gamma ||\nabla \cdot (u - \widetilde{\widetilde{v}})||^2 + \int_\Omega \frac{\delta^2}{2} |\nabla (u - \widetilde{\widetilde{v}})|^2 dx + \frac{1}{2} ||u - \widetilde{v}||^2 + \frac{1}{2} \int_\Omega \delta^2 |\nabla (u - \widetilde{U})|^2 dx.$$

The triangle inequality (and dropping the second tilde in $\widetilde{\widetilde{v}}$ in the final infimum) completes the proof. ☐

We now prove convergence with optimal rates for $u^n - u_h^n$ and $u^n - w_h^n$.

THEOREM 5.5. *Let $0 \leq \chi \leq 1$. For u, p, and f satisfying (5.6),(5.7), and u_h^n, w_h^n given by Algorithm 5.1, we have that for Δt sufficiently small*

$$\begin{aligned}&\frac{1}{2} \left[\|u(t^l) \ - \ w_h^l\|^2 + ||u(t^l) \ - \ u_h^l\|^2 \right] + \Delta t \sum_{n=1}^{l-1} \Delta t || \frac{u(t^{n+1}) \ - u(t^n)}{\Delta t} - \frac{w_h^{n+1} \ - \ u_h^n}{\Delta t} ||^2 \\ &+ \Delta t \sum_{n=1}^{l-1} \nu \|\nabla \left(u(t^{n+1}) \ - \ w_h^{n+1} \right) \|^2 \leq \ C \, \nu \, h^{2k} |||u|||_{2,k+1}^2 + \ C \nu^{-2} \, h^{2k} \, |||u|||_{\infty,k+1}^2 \\ &+ C \, \nu^{-1} \, h^{2k+1} \left(|||u|||_{4,k+1}^4 \ + \ |||\nabla u|||_{4,0}^4 \right) + \ C \, h^{2k+2} \, \|u_t\|_{2,k+1}^2 + \ C \, \nu^{-1} \, h^{2s+2} \, |||p|||_{2,s+1}^2 \\ &+ C \Delta t^2 \left[\|u_{tt}\|_{2,0}^2 \ + \ \|f_t\|_{2,0}^2 \ + \ \nu \|\nabla u_t\|_{2,0}^2 + \nu^{-1} \|\nabla u_t\|_{4,0}^4 \ + \ \nu^{-1} |||\nabla u|||_{4,0}^4 \ + \ \nu^{-1} |||\nabla u|||_{4,0}^4 \right] \\ &+ C \frac{\chi^2}{\triangle t^2} h^{2k+2} \ \left[(\gamma + \delta^2) \, \|u\|_{\infty,k+1}^2 + \ \|u\|_{\infty,k+1}^2 \right] + C \delta^4 \frac{\chi^2}{\triangle t^2} \triangle t \sum_{n=0}^{l} ||\nabla \cdot (a(u(t^n)) \nabla u(t^n))||^2 \\ &+ C \frac{\chi^2}{\triangle t^2} \left[\gamma h^{2k} |||u|||_{2,k+1}^2 + \delta^2 h^{2k} |||u|||_{2,k+1}^2 + h^{2k+2} |||u|||_{2,k+1}^2 \right] .\end{aligned}$$

The complete and detailed proof is given in the Appendix.

REMARK 5.6. *The error estimate takes the general form:*

$$\|u(t^l) - w_h^l\| + ||u(t^l) - u_h^l\| + \left(\nu\Delta t \sum_{n=1}^{l} \|\nabla(u(t^n) - w_h^n)\|^2\right)^{1/2} \leq$$
$$\leq C(u,p,data,\nu)\left[h^k + \Delta t + \frac{\chi}{\triangle t}(\gamma h^k + h^{k+1} + \delta h^k + \delta^2)\right].$$

The final term δ^2 arises from the simple bound $|a(u)| \leq 1$ on nonlinear filter coefficient. The coefficient $a(u)$ could be small in much of the domain and thus this bound pessimistic. On the other hand, at this level of generality, any error estimate must include the case $a(u) \equiv 1$. The assumption that $\triangle t$ is small can be dropped by using a different discrete Gronwall inequality if the linearly implicit method is used in Step 1: if $b^*(w_h^{n+1}, w_h^{n+1}, v_h)$ is replaced by $b^*(w_h^n, w_h^{n+1}, v_h)$ in Step 1, see Girault and Raviart [GR79].

For Taylor-Hood elements, i.e. $k = 2$, $s = 1$, we have the following.

COROLLARY 5.7. *Under the assumptions of Theorem 5.5, with (X_h, Q_h) Taylor-Hood elements, we have*

$$\||u - w_h\||_{\infty,0} + \||u - u_h\||_{\infty,0} + \left(\nu\Delta t \sum_{n=1}^{l} \|\nabla(u^n - w_h^n)\|^2\right)^{1/2}$$
$$\leq C(u,p,data,\nu)\left[h^2 + \Delta t + \frac{\chi}{\triangle t}(\gamma h^2 + h^3 + \delta h^2 + \delta^2)\right].$$

6. Numerical Experiments. In this section, we present numerical experiments to test the algorithms presented herein. Using the Green-Taylor vortex problem, we confirm the expected convergence rates of both the nonlinear filter (in Theorem 2.5) and for the NSE. Next we consider the benchmark problem of flow around a cylinder. This is a very good test for too much numerical diffusion since over diffused approximations typically do not exhibit vortex shedding correctly. We used *FreeFEM++* [HePi] using Taylor-Hood elements (X_h = continuous piecewise quadratics and Q_h = continuous piecewise linears).

6.1. Test of the Error in Nonlinear Filtering. We begin by testing the predicted error and convergence rates of Theorem 2.5 in linear vs nonlinear filtering in some 2d flows with known exact solution. In 2d helicity is exactly zero. Thus, we consider the other cases of Section 3:

$$\text{Linear Filtering} \Leftrightarrow a(\cdot) \equiv 1,$$
$$\text{Nonlinear Filtering by Q-criterion} \Leftrightarrow a = a_Q(\cdot)$$
$$\text{Nonlinear Filtering by Vreman's formula} \Leftrightarrow a = a_V(\cdot)$$
$$\text{Nonlinear Filtering by Synthesis} \Leftrightarrow a = \sqrt{(a_Q a_V)(\cdot)}.$$

For the test we select the velocity field given by the Green-Taylor vortex, [GT37], [T23], frozen at time $t = 1$. The Green Taylor vortex is used as a numerical test in many papers, e.g., Chorin [Cho68], Tafti [Tafti], John and Layton [JL02], Barbato, Berselli and Grisanti [BBG07] and Berselli [B05]. The exact velocity field is given by

$$\begin{aligned} u_1(x,y,t) &= -\cos(\omega\pi x)\sin(\omega\pi y)e^{-2\omega^2\pi^2 t/\tau}, \\ u_2(x,y,t) &= \sin(\omega\pi x)\cos(\omega\pi y)e^{-2\omega^2\pi^2 t/\tau}, \\ p(x,y,t) &= -\frac{1}{4}(\cos(2\omega\pi x) + \cos(2n\pi y))e^{-2\omega^2\pi^2 t/\tau}. \end{aligned} \tag{6.1}$$

We take

$$\omega = 1, t = 1 \text{ (fixed)}, \tau = Re = 100, \Omega = (0,1)^2, \delta = h = 1/m \tag{6.2}$$

where m is the number of subdivisions of the interval $(0, 1)$. Convergence rates are calculated from the error at two successive values of h in the usual manner by postulating $e(h) = Ch^{\beta}$ and solving for β via $\beta = \ln(e(h_1)/e(h_2))/\ln(h_1/h_2)$. The boundary conditions could be taken to be periodic (the easier case), but instead we take the boundary condition on the filtering problem to be inhomogeneous Dirichlet

$$\overline{u}^h = u_{exact}, \text{ on } \partial\Omega.$$

The errors and rates of convergence for $||u_{exact} - \overline{u}^h||$ are presented for the 4 methods in Table 6.1. All discrete filters achieve their predicted rates of convergence.

We also give a plot of the level curves of the scalar function $a(u)$ for the three nonlinear filters. Here we observe that for this simple solution the Q-criterion indicator, seems to be more selective than the Vreman indicator; only small regions of the (laminar) flow are selected for filtering. The Vreman based indicator's selectivity is also good for this special NSE solution but not as sharp.

$a(u) =$	1	1	Q-based	Q-based
h, α	$\|u_{exact} - \overline{u}^h\|_1$	rate	$\|u_{exact} - \overline{u}^h\|_1$	rate
$\frac{1}{4}$	7.110E-2	-	2.223E-1	-
$\frac{1}{8}$	3.541E-2	1.01	8.156E-2	1.45
$\frac{1}{16}$	1.123E-2	1.66	1.385E-2	2.56
$\frac{1}{32}$	2.309E-3	2.28	1.892E-3	2.87
$\frac{1}{64}$	4.209E-4	2.46	8.560E-4	1.14
$\frac{1}{128}$	7.927E-5	2.41	2.131E-4	2.01
$\frac{1}{192}$	3.022E-5	2.38	9.449E-5	2.01
$a(u) =$	Vreman-based	Vreman-based	VQ-based	VQ-based
h, α	$\|u_{exact} - \overline{u}^h\|_1$	rate	$\|u_{exact} - \overline{u}^h\|_1$	rate
$\frac{1}{4}$	1.882E-1	-	2.513E-1	-
$\frac{1}{8}$	7.202E-1	1.39	6.162E-2	2.03
$\frac{1}{16}$	1.603E-2	2.17	1.463E-2	2.07
$\frac{1}{32}$	3.535E-3	2.18	3.532E-3	2.05
$\frac{1}{64}$	8.098E-4	2.13	8.656E-4	2.03
$\frac{1}{128}$	1.958E-4	2.05	2.143E-4	2.01
$\frac{1}{192}$	8.486E-5	2.06	9.490E-5	2.01

TABLE 6.1
Errors and convergence rates for the different filters for numerical experiment 1.

6.2. Convergence Rate Verification for the Full Algorithm. Our second experiment is designed to test (and does confirm) the expected convergence rates for Algorithm 5.1 (using the CN method for Step 1) for the NSE. The prescribed solution is (6.1) above with time now no longer frozen. When the relaxation time $\tau = Re$, this is a solution of the NSE with $f = 0$, consisting of an $\omega \times \omega$ array of oppositely signed vortices that decay as $t \to \infty$. In addition to (6.2) above, we further select

$$\chi = \triangle t, \; T_{final} = 0.1, \; Re = 10, \delta = \triangle x.$$

Based on Test 1 we select as indicator function

$$\text{Linear Filtering} \Leftrightarrow a(\cdot) \equiv 1,$$

$$\text{Nonlinear Filtering by Vreman-based indicator} \Leftrightarrow a_V(u) = \sqrt{\frac{B(u)}{|\nabla u|_F^4}}.$$

From Table 6.2 we observe the expected convergence rates for both the linear and nonlinear filter are indeed found.

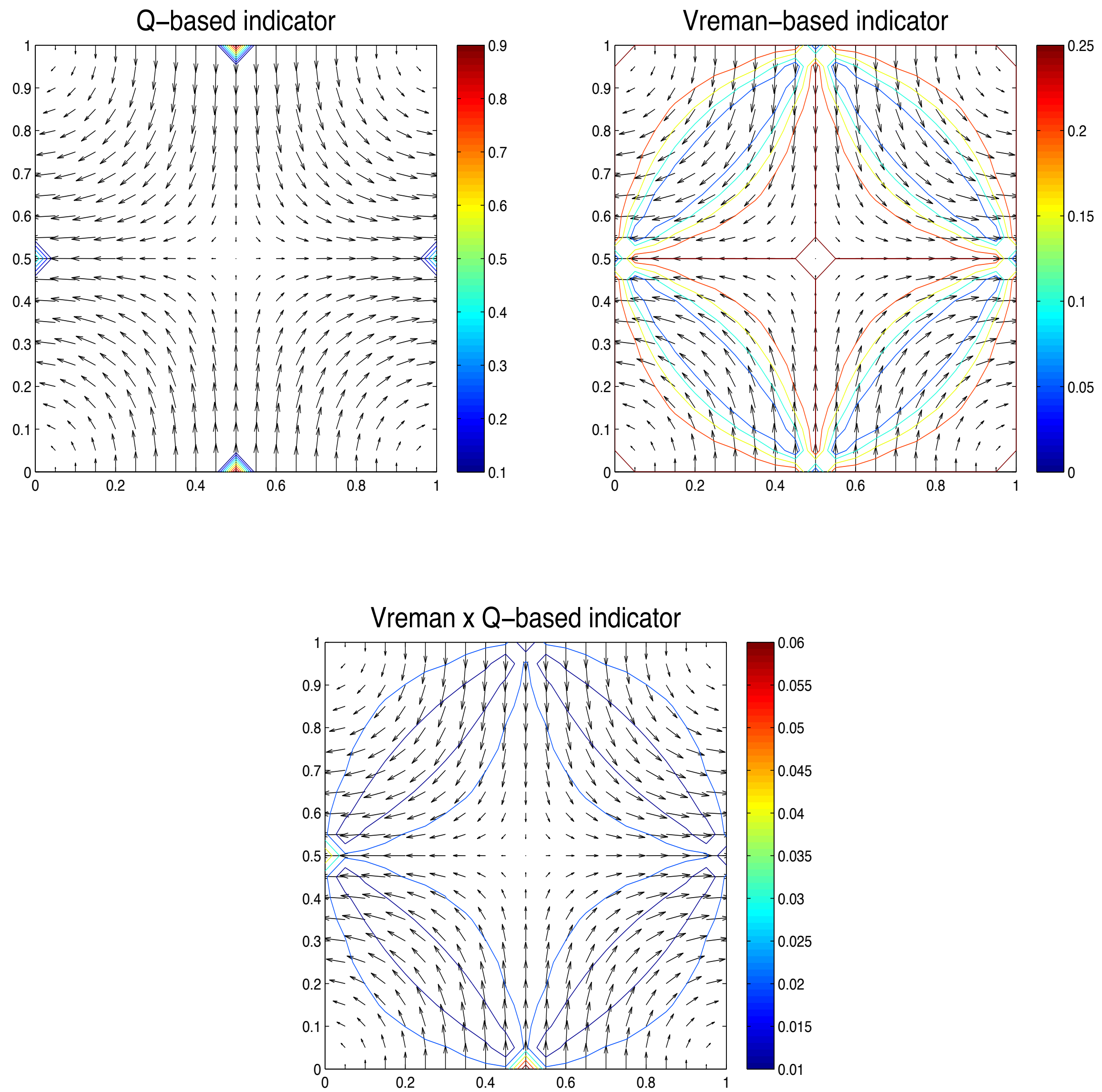

FIG. 6.1. *Shown above are contour plots of the indicator function $a(u)$ arising from filtering with the Q-based, Vreman based, and Q-Vreman composition nonlinear filters, overlaying the velocity vector field.*

6.3. Flow around a cylinder. Our next numerical illustration is for two dimensional under-resolved channel flow around a cylinder. We compute values for the maximal drag $c_{d,max}$ and lift $c_{l,max}$ coefficient at the cylinder, and for the pressure difference $\Delta p(t)$ between the front and back of the cylinder at the final time $T = 8$. This is a well known benchmark problem taken from Shäfer and Turek [ST96] and John [J04]. It is not turbulent but does have interesting features. The flow patterns are driven by the interaction of a fluid with a wall which is an important scenario for industrial flows. This simple flow is actually quite difficult to simulate successfully by a model with sufficient regularization to handle higher Reynolds number problems.

The domain for the problem is a 2.2×0.41 rectangular channel with a cylinder of radius 0.05 centered at $(0.2, 0.2)$ (taking the bottom left corner of the rectangle as the origin). The cylinder, top and bottom of

	$a(u) =$	1	1	Vreman-based	Vreman-based
Δt	h, α	$\Vert u_{NSE} - w_h \Vert_{2,1}$	rate	$\Vert u_{NSE} - w_h \Vert_{2,1}$	rate
0.005	$\frac{1}{4}$	6.300E-2	-	6.382E-2	-
$\frac{0.005}{2}$	$\frac{1}{8}$	1.558E-2	2.01	1.556E-2	2.04
$\frac{0.005}{4}$	$\frac{1}{16}$	3.814E-3	2.03	3.638E-3	2.10
$\frac{0.005}{8}$	$\frac{1}{32}$	9.844E-4	1.95	8.803E-4	2.05
$\frac{0.005}{16}$	$\frac{1}{64}$	2.480E-4	1.99	2.175E-4	2.02

TABLE 6.2

Errors and convergence rates for Algorithm 5.1 using the linear filter and the nonlinear filter with Vreman-based indicator, for numerical experiment 2.

the channel are prescribed no slip boundary conditions, and the time dependent inflow and outflow profile are

$$u_1(0, y, t) = u_1(2.2, y, t) = \frac{6}{0.41^2} \sin(\pi\, t/8) y(0.41 - y)\,,$$
$$u_2(0, y, t) = u_2(2.2, y, t) = 0.$$

The viscosity is set as $\nu = 10^{-3}$ and the external force $f = 0$. The Reynolds number of the flow, based on the diameter of the cylinder and on the mean velocity inflow is $0 \le Re \le 100$.

For this setting, it is expected that as the flow increases from time $t = 2$ to $t = 4$ two vortices start to develop behind the cylinder. They then separate into the flow, and soon after a vortex street forms which can be visible through the final time $t = 8$. This evolution can be seen in Figure 6.2, where the velocity field and speed contours are plotted at $t = 2,\ 4,\ 6$ and 8 for a fully resolved solution. Lift and drag coefficients (using the one dimensional method described by V. John [J04]) for fully resolved flows will lie in the reference intervals ([ST96])

$$c_{d,max}^{ref} \in [2.93,\ 2.97], \quad c_{l,max}^{ref} \in [0.47,\ 0.49], \quad \Delta p^{ref} \in [-0.115,\ -0.105]$$

A mesh providing 14,401 total degrees of freedom with (P_2, P_1) elements, a time step of $\Delta t = 0.0025$, and filtering radius δ chosen to be the average mesh width, is used for all simulations, for a clear comparison of the different algorithms. These simulations are all under-resolved; fully resolved computations use upwards of 100,000 degrees of freedom and even smaller time steps. Thus we do not expect exact agreement with solutions of Algorithm 5.1 with the true solution or lift and drag reference values. However, we do expect answers to be close, in order for the algorithm to be a useful 'model'.

We test Algorithm 5.1, here with a Crank-Nicolson temporal discretization, with the following options for the filter.

$$\text{Linear Filtering} \Leftrightarrow a(\cdot) \equiv 1,$$
$$\text{Nonlinear Filtering by Q-criterion} \Leftrightarrow a = a_Q(\cdot)$$
$$\text{Nonlinear Filtering by Vreman's formula} \Leftrightarrow a = a_V(\cdot)$$
$$\text{Nonlinear Filtering by Synthesis} \Leftrightarrow a = a_{VQ} = \sqrt{(a_Q a_V)(\cdot)}.$$

Algorithm 5.1 (with CN in Step 1) performs well for each of the three nonlinear filters, but is significantly less accurate for the linear filter case. Plots of each of the solutions' velocity fields are given in Figure 6.3, and comparing to the resolved solutions in Figure 6.2, we see that the three solutions from $a_Q,\ a_V,\ a_{VQ}$ all match the resolved solution well (*for such a coarse mesh approximation*). However, the solution from using $a(u) = 1$ does not capture the full vortex street; near the end of the channel it is clearly not resolved. We also see from the lift and drag calculations, given in Table 6.3, that the solutions from the $a_Q,\ a_V,\ a_{VQ}$ filters give reasonable approximations to lift, drag and pressure drop. The solution from $a(u) = 1$, on the other hand, gives a poor approximation of the lift coefficient.

7. Conclusions. Nonlinear filtering, properly done, at each step stabilizes marginally resolved scales and does *not* over diffuse. For *linear* filtering $w - \overline{w}$ is very small in regions where w is smooth. For a

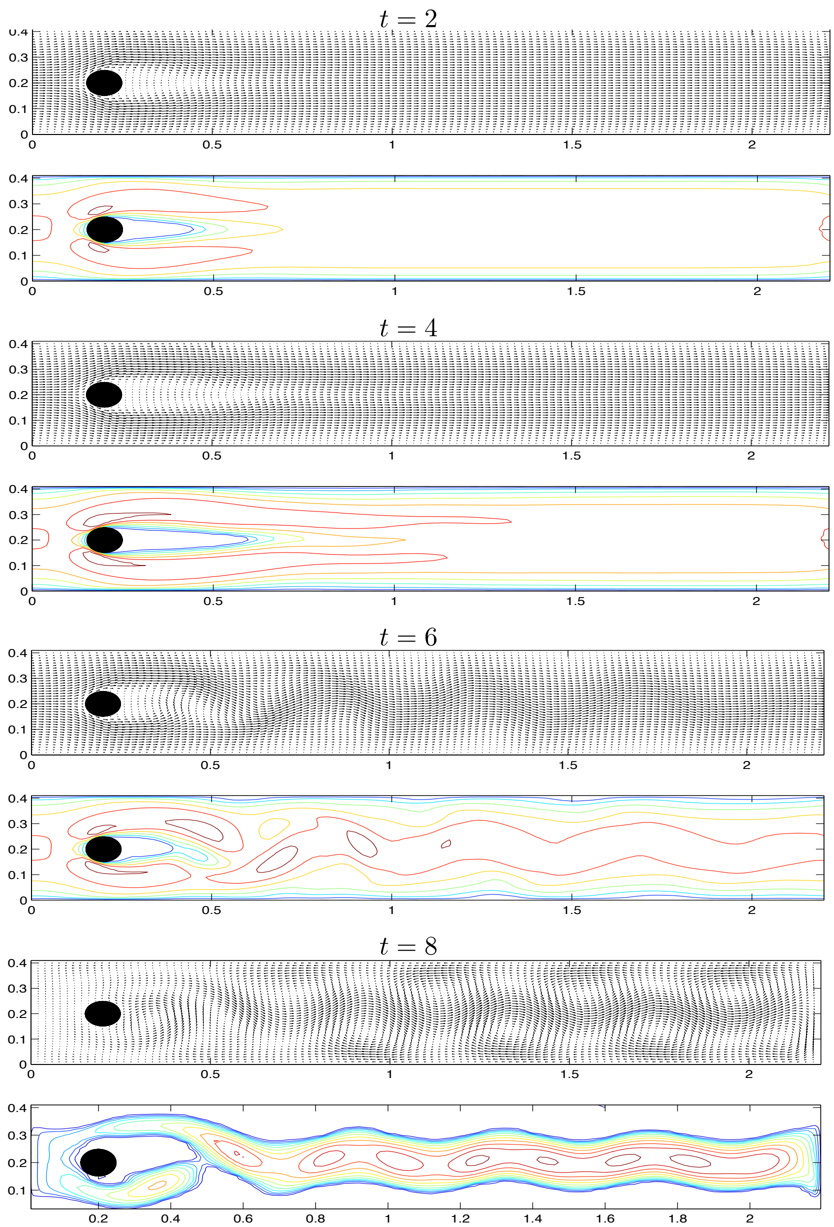

FIG. 6.2. *Shown above is the development of the vortex street for flow the $\nu = 0.001$ flow around a cylinder benchmark problem. The velocity field and speed contours are plotted at $t = 2,\ 4,\ 6,\ 8$. This plot is for a fully resolved solution.*

Filter	$c_{d,max}$	$c_{l,max}$	Δp
$a(u) = 1$	2.898	0.151	-0.113
$a(u) = a_V(u)$	2.895	0.542	-0.115
$a(u) = a_Q(u)$	2.892	0.551	-0.114
$a(u) = a_{VQ}(u)$	2.892	0.558	-0.114

TABLE 6.3
Lift, drag and pressure drop for the flow around a cylinder experiment with the four different filters.

properly chosen indicator function for *nonlinear* filtering, $w - \overline{w}$ is very small not only in smooth regions, but also in regions of persistent eddies, coherent flow structures which are not broken down rapidly and as well as in laminar regions. Thus nonlinear filtering reduces both numerical errors and turbulence modeling

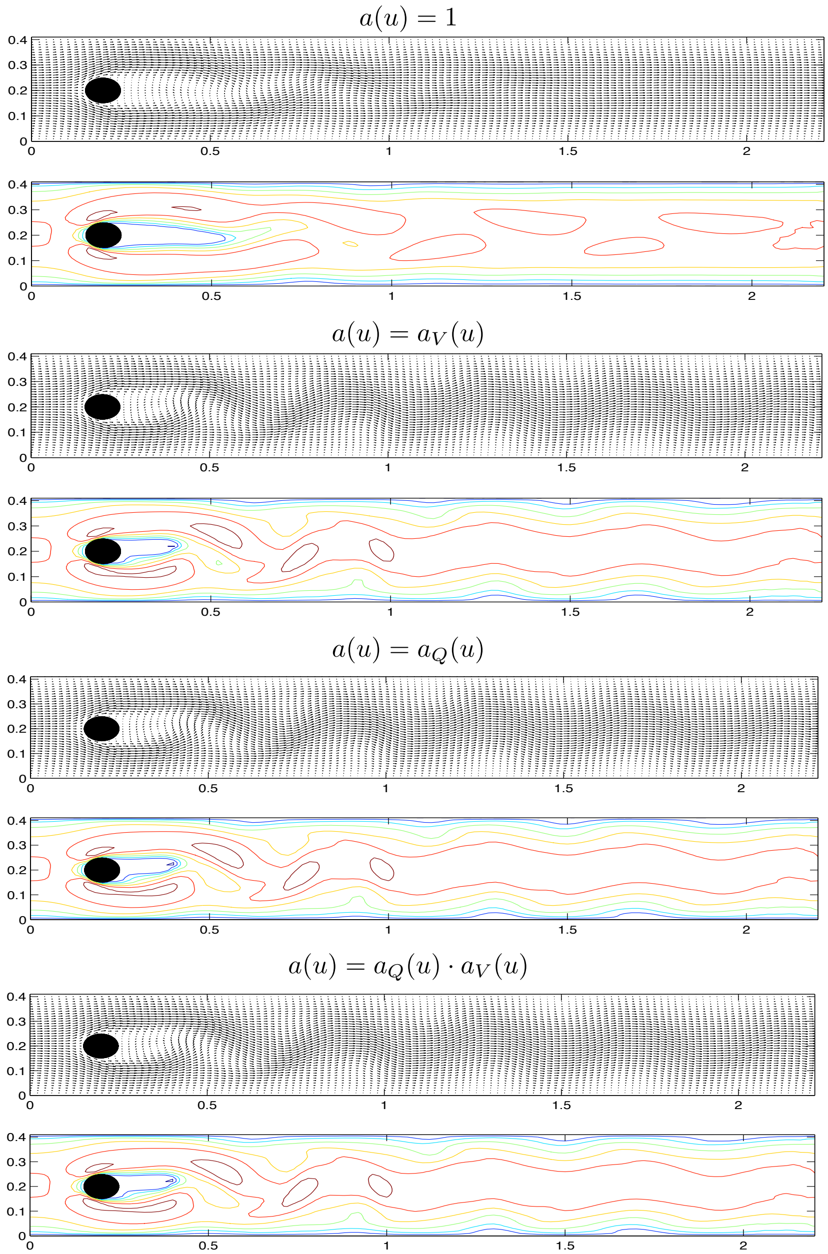

FIG. 6.3. *Shown above is the velocity field and speed contours for the benchmark cylinder problem at $t = 6$, for the four different filter choices. Comparing to the resolved solution in Figure 6.2, we see the solution from using $a(u) = 1$ does not capture the vortex street, while the other three methods do and match the fully resolved solution well.*

errors. It reduces model dissipation selectively so that it *more closely mimics the exact physics of the energy cascade*. Nonlinear filtering reduces implementing a complex, nonlinear turbulence model into a flow code (possibly a legacy code of great length) to providing a function subroutine and solving one well conditioned, SPD linear system each time step. It also gives a general approach to increasing the accuracy of turbulence models. The definition of nonlinear filters via differential filters is the clearest mathematically but possibly not the most efficient. The extension of the idea to filtering by local averaging with locally and nonlinearly varying averaging radius, taking the work herein as a first step, is an interesting extension of importance to many practical flow simulations.

REFERENCES

[AL99] N.A. Adams and A. Leonard, *Deconvolution of subgrid scales for the simulation of shock-turbulence interaction*, p. 201 in: *Direct and Large Eddy Simulation III*, (eds.: P. Voke, N.D. Sandham and L. Kleiser), Kluwer, Dordrecht, 1999.

[AS02] N.A. Adams and S. Stolz, *A subgrid-scale deconvolution approach for shock capturing*, J.C.P., 178 (2002), 391-426.

[AS01] N. A. Adams and S. Stolz, *Deconvolution methods for subgrid-scale approximation in large eddy simulation*, Modern Simulation Strategies for Turbulent Flow, R.T. Edwards, 2001.

[B76] G. Baker, *Galerkin Approximations for the Navier-Stokes Equations*, technical report, Harvard University, August, 1976.

[BBG07] D. Barbato, L.C. Berselli, and C.R. Grisanti, *Analytical and numerical results for the rational large eddy simulation model*, J. Math. Fluid Mech., 9 (2007), 44-74.

[B05] L.C. Berselli, *On the large eddy simulation of the Taylor-Green vortex*, J. Math. Fluid Mech., 7 (2005), S164-S191.

[BIL04] L.C. Berselli, T. Iliescu and W. Layton, *Large Eddy Simulation*, Springer, Berlin, 2004

[B61] R. Betchov, *Semi-isotropic turbulence and helicoidal flows*, Phys. Fluids, 4(1961) 925-926.

[BIR09] J. Borggaard, T. Iliescu and J.P. Roop, *A Bounded Artificial Viscosity Large Eddy Simulation Model*, SIAM J. Numer. Anal., 47(2009), 622-645.

[Boyd98] J.P. Boyd, *Two comments on filtering for Chebyshev and Legendre spectral and spectral element methods : Preserving the boundary conditions and interpretation of the filter as a diffusion*, J. Comp. Phys., 143 (1998), 283–288.

[BS94] S. Brenner and L.R. Scott, *The Mathematical Theory of Finite Element Methods*, Springer-Verlag, 1994.

[Cho68] A.J. Chorin, *Numerical solution for the Navier-Stokes equations*, Math. Comp., 22 (1968), 745-762.

[CL08] J. Connors and W. Layton, *On the accuracy of the finite element method plus time relaxation*, Math. Comp.,to appear, 2008.

[DF02] C. Doering and C. Foias, *Energy dissipation in body-forced turbulence*, J. Fluid Mech., 467 (2002), 289-306.

[D04] A. Dunca, *Space averaged Navier-Stokes equations in the presence of walls*, PhD Thesis, University of Pittsburgh, 2004.

[D02] A. Dunca, *Investigation of a shape optimization algorithm for turbulent flows*, report ANL/MCS-P1101-1003, Argonne National Lab, 2002, http://www-fp.mcs.anl.gov/division/publications/.

[DE04] A. Dunca and Y. Epshteyn, *On the Stolz-Adams de-convolution LES model*, SIAM J. Math. Anal., 37 (2006), 1890-1902.

[ELN07] V. Ervin, W. Layton and M. Neda , *Numerical analysis of a higher order time relaxation model of fluids*, Int. J. Numer. Anal. and Modeling, 4 (2007), 648-670.

[ELN10] V. Ervin, W. Layton and M. Neda, *Numerical analysis of filter based stabilization for evolution equations*, technical report, TR-MATH 10-01, 2010, http://www.mathematics.pitt.edu/research/technical-reports.php.

[FM01] P. Fischer and J. Mullen, *Filter-based stabilization of spectral element methods*, C. R. Acad. Sci. Paris, 332(1), 265 (2001).

[G89] M.D. Gunzburger, *Finite Element Methods for Viscous Incompressible Flows - A Guide to Theory, Practices, and Algorithms*, Academic Press, 1989.

[Geu97] B. J. Geurts, *Inverse modeling for large eddy simulation*, Phys. Fluids, 9 (1997), 3585.

[Ga00] G. P. Galdi, *Lectures in Mathematical Fluid Dynamics*, Birkhauser-Verlag, 2000.

[Gal94] G.P. Galdi, *An introduction to the Mathematical Theory of the Navier-Stokes equations, Volume I*, Springer, Berlin, 1994.

[GAS09] E. Garnier, N. Adams and P. Sagaut, *Large eddy simulation for compressible flows*, Springer, Berlin, 2009.

[Ger86] M. Germano, *Differential filters of elliptic type*, Phys. Fluids, 29 (1986), 1757-1758.

[GR79] V. Girault, P.-A. Raviart , *Finite Element Approximation of the Navier-Stokes Equations*, Springer, Verlag; Berlin, 1979.

[GT37] A.E. Green and G.I. Taylor, *Mechanism of the production of small eddies from larger ones*, Proc. Royal Soc. A, 158 (1937), 499-521.

[Gue04] R. Guenanff, *Non-stationary coupling of Navier-Stokes/Euler for the generation and radiation of aerodynamic noises*, PhD thesis: Dept. of Mathematics, Université Rennes 1, Rennes, France, 2004.

[HePi] F. Hecht and O. Pironneau, *FreeFEM++* , webpage: http://www.freefem.org.

[HeRa] J.G. Heywood and R. Rannacher, *Finite element approximation of the nonstationary Navier-Stokes problem. Part IV: Error analysis for second-order time discretization*, SIAM J. Numer. Anal., 2 (1990), 353-384.

[HWM88] J.C. Hunt, A.A. Wray and P. Moin, *Eddies stream and convergence zones in turbulent flows*, CTR report CTR-S88, 1988.

[J04] V. John, *Reference values for drag and lift of a two-dimensional time-dependent flow around the cylinder,* International Journal for Numerical Methods in Fluids, 44 (2004), 777-788.

[JL02] V. John and W. Layton, *Analysis of Numerical Errors in Large Eddy Simulation*, SIAM J. Numer. Anal., 40 (2002), 995-1020.

[Lad69] O. Ladyzhenskaya, *The Mathematical Theory of Viscous Incompressible Flow*, Gordon and Breach, 1969.

[L07] W Layton, *A remark on regularity of an elliptic-elliptic singular perturbation problem,* technical report, http://www.mathematics.pitt.edu/research/technical-reports.php, 2007.

[L07b] W. Layton , *Superconvergence of finite element discretization of time relaxation models of advection*, BIT, 47 (2007), 565-576.

[LMNOR09] W. Layton, C. Manica, M. Neda, M. Olshanskii and L. Rebholz, *On the accuracy of the rotation form in simulations of the Navier-Stokes equations*, Journal of Computational Physics, 228(9), 3433-3447, 2009.

[LMNR06] W. Layton, C. Manica, M. Neda and L. Rebholz, *The joint Helicity-Energy cascade for homogeneous, isotropic turbulence generated by approximate deconvolution models,* Adv. and Appls. in Fluid Mechanics, 4 (2008), 1-46.

[LN07] W. Layton and M. Neda, *Truncation of scales by time relaxation*, JMAA, 325 (2007), 788-807.

[LT83] E. Levich and A. Tsinober, *On the role of helical structures in 3-dimensional turbulent flows*, Physics Letters 93A (1983) 293-297.

[LT83b] E. Levich and A. Tsinober, *Helical structures, fractal dimensions and renormalization group approach in homogeneous turbulence*, Physics Letters 96A (1983) 292-297.

[Lilly86] D.K. Lilly, *The structure, energetics and propagation of rotating convection storms, II: Helicity and Storm Stabilization*, J Atmos. Sciences, 43(1986),126-140.

[MKM06] C. Manica and S. Kaya Merdan, *Convergence analysis of the finite element method for a fundamental model in turbulence*, Technical Report, University of Pittsburgh, 2006.

[MLF03] J. Mathew, R. Lechner, H. Foysi, J. Sesterhenn and R. Friedrich, *An explicit filtering method for large eddy simulation of compressible flows*, Physics of Fluids, 15 (2003), 2279-2289.

[MF98] J.S. Mullen and P.F. Fischer, *Filtering techniques for complex geometry fluid flows*, Comm. in Num. Meth. in Eng., 15 (1999), 9-18.

[R89] Ph. Rosenau, *Extending hydrodynamics via the regularization of the Chapman-Enskog expansion*, Phys. Rev. A, 40 (1989), 7193.

[S01] P. Sagaut, *Large eddy simulation for Incompressible flows,* Springer, Berlin, 2001.

[ST92] S. Schochet and E. Tadmor, *The regularized Chapman-Enskog expansion for scalar conservation laws*, Arch. Rat. Mech. Anal. 119 (1992), 95.

[ST96] M. Shäfer and S. Turek, *Benchmark computations of laminar flow around cylinder,* in: Flow Simulation with High-Performance Computers II, Vieweg, 1996.

[S07] I. Stanculescu, *Existence Theory of Abstract Approximate Deconvolution Models of Turbulence,* Annali dell'Universitá di Ferrara, 54 (2008), 145-168.

[SAK01a] S. Stolz, N.A. Adams and L. Kleiser, *The approximate deconvolution model for LES of compressible flows and its application to shock-turbulent-boundary-layer interaction*, Phys. Fluids, 13 (2001), 2985.

[SAK01b] S. Stolz, N.A. Adams and L. Kleiser, *An approximate deconvolution model for large eddy simulation with application to wall-bounded flows*, Phys. Fluids, 13 (2001), 997.

[SAK02] S. Stolz, N.A. Adams and L. Kleiser, *The approximate deconvolution model for compressible flows: isotropic turbulence and shock-boundary-layer interaction*, in: Advances in LES of complex flows (editors: R. Friedrich and W. Rodi) Kluwer, Dordrecht, 2002

[SA99] S. Stolz and N.A. Adams, *On the approximate deconvolution procedure for LES*, Phys. Fluids, II (1999), 1699-1701.

[Tafti] D. Tafti, *Comparison of some upwind-biased high-order formulations with a second order central-difference scheme for time integration of the incompressible Navier-Stokes equations*, Comput. & Fluids, 25 (1996), 647-665.

[T23] G.I. Taylor, *On decay of vortices in a viscous fluid*, Phil. Mag., 46 (1923), 671-674.

[TL83] A. Tsinober and E. Levich, *On the helical nature of 3-dimensional coherent structures in turbulent flows*, Physics Letters 99A (1983) 321-324.

[VR02] M.R. Visbal and D.P. Rizzetta, *Large eddy simulation on curvilinear grids using compact differencing and filtering schemes*, J. Fluids Eng. 124 (2002) 836-847.

[V04] A.W. Vreman, *An eddy-viscosity subgrid-scale model for turbulent shear flow: algebraic theory and applications,* Phys. Fluids 16 (2004), 3670-3681.

[W97] X. Wang, *The time averaged energy dissipation rates for shear flows*, Physica D, 99 (2004), 555-563.

Appendix. The Proof of Theorem 5.5.

Proof. At time t^{n+1}, the true solution of the NSE u satisfies

$$(u^{n+1}-u^n, v_h) + \Delta t\nu(\nabla u^{n+1}\,,\nabla v_h) + \Delta t\, b^*(u^{n+1}\,, u^{n+1}\,, v_h) \;-\; \Delta t\,(p^{n+1}, \nabla\cdot v_h) = \Delta t\,(f^{n+1}, v_h) \;+\; \Delta t\, Intp(u^{n+1}; v_h)\;, \tag{A.1}$$

for all $v_h \in V_h$, where $Intp(u^n; v_h)$, representing the interpolating error, denotes

$$Intp(u^n; v_h) = \big((u^{n+1}-u^n)/\Delta t - u_t^{n+1}, v_h\big)\;.$$

We let

$$\varepsilon^n \;=\; u^n \,-\, w_h^n, e^n \;=\; u^n \,-\, u_h^n\;.$$

Subtracting Step 1 of the algorithm from (A.1), we have

$$(\varepsilon^{n+1}-e^n, v_h) \;+\; \Delta t\,\nu(\nabla\varepsilon^{n+1}\,, \nabla v_h) = -\Delta t b^*(u^{n+1}\,, u^{n+1}\,, v_h) \;+\; \Delta t\, b^*(w_h^{n+1}, w_h^{n+1}, v_h) + \Delta t(p^{n+1}, \nabla\cdot v_h) \;+\; \Delta t\, Intp(u^{n+1}; v_h)\;, \tag{A.2}$$

for all $v_h \in V_h$. Let $U^n \in V_h$ be an approximation to $u^n = u(t_n)$. Split the errors as

$$\begin{aligned} \varepsilon^n &= u^n - w_h^n = (u^n - U^n) + (U^n - w_h^n) := \eta^n + \psi_h^n, \\ e^n &= u^n - u_h^n = (u^n - U^n) + (U^n - u_h^n) := \eta^n + \phi_h^n. \end{aligned}$$

Choose $v_h = \psi_h^{n+1}$, use $(\nabla \cdot \psi_h^{n+1}, q_h) = 0, \quad \forall q_h \in Q_h$, and note that by the polarization identity

$$(\phi_h^n, \psi_h^{n+1}) = \frac{1}{2}\left(\|\psi_h^{n+1}\|^2 + \|\phi_h^n\|^2\right) - \frac{1}{2}||\psi_h^{n+1} - \phi_h^n||^2.$$

Equation (A.2) then becomes

$$\begin{aligned} &\frac{1}{2}\left(\|\psi_h^{n+1}\|^2 - \|\phi_h^n\|^2\right) + \frac{1}{2}||\psi_h^{n+1} - \phi_h^n||^2 + \Delta t\, \nu \|\nabla \psi_h^{n+1}\|^2 \\ &= -(\eta^{n+1} - \eta^n, \psi_h^{n+1}) - \Delta t\, \nu (\nabla \eta^{n+1}, \nabla \psi_h^{n+1}) \\ &\quad - \Delta t\, b^*(u^{n+1}, u^{n+1}, \psi_h^{n+1}) + \Delta t\, b^*(w_h^{n+1}, w_h^{n+1}, \psi_h^{n+1}) \\ &\quad + \Delta t (p^{n+1} - q_h, \nabla \cdot \psi_h^{n+1}) + \Delta t\, Intp(u^{n+1}; \psi_h^{n+1})\,. \end{aligned} \tag{A.3}$$

Next we estimate the terms on the RHS of (A.3).

$$\begin{aligned} (\eta^{n+1} - \eta^n, \psi_h^{n+1}) &\leq \frac{1}{2}\Delta t \|\frac{\eta^{n+1} - \eta^n}{\Delta t}\|^2 + \frac{1}{2}\Delta t \|\psi_h^{n+1}\|^2 \\ &= \frac{1}{2}\Delta t \int_\Omega \left(\frac{1}{\Delta t}\int_{t^n}^{t^{n+1}} \eta_t dt\right)^2 d\Omega + \frac{1}{2}\Delta t \|\psi_h^{n+1}\|^2 \\ &\leq \frac{1}{2}\int_{t^n}^{t^{n+1}} \|\eta_t\|^2\, dt + \frac{1}{2}\Delta t\left(\|\psi_h^{n+1}\|^2 + \|\phi_h^n\|^2\right). \end{aligned} \tag{A.4}$$

$$\nu(\nabla \eta^{n+1}, \nabla \psi_h^{n+1}) \leq \frac{\nu}{10}\|\nabla \psi_h^{n+1}\|^2 + C\nu \|\nabla \eta^{n+1}\|^2\,. \tag{A.5}$$

We rewrite $b^*(u^{n+1}, u^{n+1}, \psi_h^{n+1}) - b^*(w_h^{n+1}, w_h^{n+1}, \psi_h^{n+1})$ and use $b^*(w_h^{n+1}, \psi_h^{n+1}, \psi_h^{n+1}) = 0$ to give

$$\begin{aligned} &b^*(u^{n+1}, u^{n+1}, \psi_h^{n+1}) - b^*(w_h^{n+1}, w_h^{n+1}, \psi_h^{n+1}) \\ &= b^*(u^{n+1}, u^{n+1}, \psi_h^{n+1}) - b^*(w_h^{n+1}, u^{n+1}, \psi_h^{n+1}) \\ &\quad + b^*(w_h^{n+1}, u^{n+1}, \psi_h^{n+1}) - b^*(w_h^{n+1}, w_h^{n+1}, \psi_h^{n+1}) \\ &= b^*(\varepsilon^{n+1}, u^{n+1}, \psi_h^{n+1}) + b^*(w_h^{n+1}, \varepsilon^{n+1}, \psi_h^{n+1}) \\ &= b^*(\eta^{n+1} + \psi_h^{n+1}, u^{n+1}, \psi_h^{n+1}) + b^*(w_h^{n+1}, \eta^{n+1} + \psi_h^{n+1}, \psi_h^{n+1}) \\ &= b^*(\eta^{n+1}, u^{n+1}, \psi_h^{n+1}) + b^*(\psi_h^{n+1}, u^{n+1}, \psi_h^{n+1}) + b^*(w_h^{n+1}, \eta^{n+1}, \psi_h^{n+1})\,. \end{aligned} \tag{A.6}$$

Using $b^*(u, v, w) \leq C(\Omega)\sqrt{\|u\|\,\|\nabla u\|}\,\|\nabla v\|\,\|\nabla w\|$, for $u,\ v,\ w \ \in X$, and Young's inequality, we bound the terms on the RHS of (A.6) as follows.

$$\begin{aligned} b^*(\eta^{n+1}, u^{n+1}, \psi_h^{n+1}) &\leq C\sqrt{\|\eta^{n+1}\|\,\|\nabla \eta^{n+1}\|}\,\|\nabla u^{n+1}\|\,\|\nabla \psi_h^{n+1}\| \\ &\leq \frac{\nu}{10}\|\nabla \psi_h^{n+1}\|^2 + C\,\nu^{-1}\|\eta^{n+1}\|\,\|\nabla \eta^{n+1}\|\,\|\nabla u^{n+1}\|^2 \end{aligned} \tag{A.7}$$

$$\begin{aligned} b^*(\psi_h^{n+1}, u^{n+1}, \psi_h^{n+1}) &\leq C\,\|\psi_h^{n+1}\|^{1/2}\,\|\nabla \psi_h^{n+1}\|^{3/2}\,\|\nabla u^{n+1}\| \\ &\leq \frac{\nu}{10}\|\nabla \psi_h^{n+1}\|^2 + C\,\nu^{-3}\|\nabla u^{n+1}\|^4\left(\|\psi_h^{n+1}\|^2 + \|\phi_h^{n+1}\|^2\right) \end{aligned} \tag{A.8}$$

$$b^*(w_h^{n+1}, \eta^{n+1}, \psi_h^{n+1}) \le C\,\|\nabla w_h^{n+1}\|\,\|\nabla \eta^{n+1}\|\,\|\nabla \psi_h^{n+1}\|$$
$$\le \frac{\nu}{10}\,\|\nabla \psi_h^{n+1}\|^2 \;+\; C\,\nu^{-1}\,\|\nabla w_h^{n+1}\|^2\,\|\nabla \eta^{n+1}\|^2 \tag{A.9}$$

$$(p^{n+1} - q_h, \nabla\cdot\psi_h^{n+1}) \le \|p^{n+1} - q_h\|\,\|\nabla\cdot\psi_h^{n+1}\|$$
$$\le \frac{\nu}{10}\|\nabla\psi_h^{n+1}\|^2 \;+\; C\,\nu^{-1}\,\|p^{n+1} - q_h\|^2\,. \tag{A.10}$$

With the bounds (A.4)–(A.10), (A.3) becomes

$$\begin{aligned}
&\frac{1}{2}\left(\|\psi_h^{n+1}\|^2 \;-\; \|\phi_h^n\|^2\right) + \frac{1}{2}\|\psi_h^{n+1} - \phi_h^n\|^2 + \Delta t\,\frac{\nu}{2}\|\nabla\psi_h^{n+1}\|^2 \\
&\le\; C\Delta t\,(1 + \nu^{-3}\|\nabla u^{n+1}\|^4)\|\left(\|\psi_h^{n+1}\|^2 \;+\; \|\phi_h^{n+1}\|^2\right) \;+\; C\nu\Delta t\|\nabla\eta^{n+1}\|^2 \\
&\quad + C\Delta t\,\|\nabla w_h^{n+1}\|^2\,\|\nabla\eta^{n+1}\|^2 + C\nu^{-1}\Delta t\,\|\nabla u^{n+1}\|^2\|\eta^{n+1}\|\,\|\nabla\eta^{n+1}\| \\
&\quad + C\int_{t^{n-1}}^{t^n}\|\eta_t\|^2\,dt \;+\; C\,\Delta t\,\nu^{-1}\|p^{n+1} - q_h\|^2 \;+\; \Delta t\,|Intp(u^n;\psi_h^{n+1})|.
\end{aligned} \tag{A.11}$$

As u_h^n and w_h^n are connected through the *filter-relax* operations in Steps 2 and 3, we next use those equations to obtain a relationship between $\|\psi_h^n\|$ and $\|\phi_h^n\|$. The true solution $u(\cdot, t^n) = u^n$ satisfies

$$u^n \;=\; (1-\chi)u^n \;+\; \chi\overline{u^n}^h \;+\; \chi\left(u^n - \overline{u^n}^h\right)\,. \tag{A.12}$$

Subtracting Step 3 of Algorithm 5.1 from (A.12) and rearranging yields

$$e^{n+1} =\; (1-\chi)\varepsilon^{n+1} \;+\; \chi\overline{\varepsilon^{n+1}}^h \;+\; \chi\left(u^{n+1} - \overline{u^{n+1}}^h\right), \text{ rewritten as:} \tag{A.13}$$
$$\phi_h^{n+1} =\; (1-\chi)\psi_h^{n+1} \;+\; \chi\overline{\psi_h^{n+1}}^h \;-\; \chi\left(\eta^{n+1} - \overline{\eta^{n+1}}^h\right) \;+\; \chi\left(u^{n+1} - \overline{u^{n+1}}^h\right).$$

Taking norms and using $||\overline{\psi_h^n}^h|| \le ||\psi_h^n||$ thus gives

$$\|\phi_h^{n+1}\| \le\; (1-\chi)\|\psi_h^{n+1}\| \;+\; \chi\,\|\psi_h^{n+1}\| \;+\; \chi\|\eta^{n+1} - \overline{\eta^{n+1}}^h\| \;+\; \chi\|u^{n+1} - \overline{u^{n+1}}^h\|,$$
$$\|\phi_h^{n+1}\| \le\; \|\psi_h^{n+1}\| \;+\; \chi\|\eta^{n+1} - \overline{\eta^{n+1}}^h\| \;+\; \chi\|u^{n+1} - \overline{u^{n+1}}^h\|. \tag{A.14}$$

This implies (shifting the index back one step to n)

$$\begin{aligned}
&\frac{1}{2}\|\phi_h^n\|^2 = \frac{1}{4}\|\phi_h^n\|^2 + \frac{1}{4}\|\phi_h^n\|^2 \\
&\le\; \frac{1}{4}\|\phi_h^n\|^2 + \frac{1}{4}\left[\|\psi_h^n\| \;+\; \chi\|\eta^n - \overline{\eta^n}^h\| + \chi\|u^n - \overline{u^n}^h\|\right]^2 \\
&\le \frac{1}{4}\left[\|\phi_h^n\|^2 + \|\psi_h^n\|^2\right] + \frac{1}{2}\left[\chi\|\eta^n - \overline{\eta^n}^h\| \;+\; \chi\|u^n - \overline{u^n}^h\|\right]\|\psi_h^n\| \\
&\qquad + \frac{1}{4}\left[\chi\|\eta^n - \overline{\eta^n}^h\| + \chi\|u^n - \overline{u^n}^h\|\right]^2 \\
&\le \frac{1}{4}\left[\|\phi_h^n\|^2 + \|\psi_h^n\|^2\right] + \frac{\chi}{2\triangle t}\left[\|\eta^n - \overline{\eta^n}^h\| \;+\; \|u^n - \overline{u^n}^h\|\right][\triangle t\|\psi_h^n\|] \\
&\qquad + \frac{\chi^2}{2}\left[\,\|\eta^n - \overline{\eta^n}^h\|^2 + \|u^n - \overline{u^n}^h\|^2\right].
\end{aligned} \tag{A.15}$$

Returning to the index $n+1$, we rearrange and square. This yields, after further manipulations,

$$\|\phi_h^{n+1}\| - \left[\chi\|\eta^{n+1} - \overline{\eta^{n+1}}^h\| \;+\; \chi\|u^{n+1} - \overline{u^{n+1}}^h\|\right] \le\; \|\psi_h^{n+1}\|\,, \text{ and thus}$$
$$\left\{\|\phi_h^{n+1}\| - \left[\chi\|\eta^{n+1} - \overline{\eta^{n+1}}^h\| \;+\; \chi\|u^{n+1} - \overline{u^{n+1}}^h\|\right]\right\}^2 \le\; \|\psi_h^{n+1}\|^2, \text{ or}$$
$$\begin{aligned}
&\|\phi_h^{n+1}\|^2 - \;2\left[\chi\|\eta^{n+1} - \overline{\eta^{n+1}}^h\| \;+\; \chi\|u^{n+1} - \overline{u^{n+1}}^h\|\right]\|\phi_h^{n+1}\| \\
&\qquad + \left[\chi\|\eta^{n+1} - \overline{\eta^{n+1}}^h\| \;+\; \chi\|u^{n+1} - \overline{u^{n+1}}^h\|\right]^2 \le\; \|\psi_h^{n+1}\|^2
\end{aligned}$$

Using this in the first term of the LHS of (A.11) and rearranging gives

$$\begin{aligned} &\frac{1}{2}\|\psi_h^{n+1}\|^2 \geq \frac{1}{4}\|\psi_h^{n+1}\|^2 + \frac{1}{4}\|\psi_h^{n+1}\|^2 \geq \\ &\geq \frac{1}{4}\|\psi_h^{n+1}\|^2 + \frac{1}{4}\{||\phi_h^{n+1}\|^2 - 2\left[\chi\|\eta^{n+1} - \overline{\eta^{n+1}}^h\| + \chi\|u^{n+1} - \overline{u^{n+1}}^h\|\right]\|\phi_h^{n+1}\| \\ &\quad + \left[\chi\|\eta^{n+1} - \overline{\eta^{n+1}}^h\| + \chi\|u^{n+1} - \overline{u^{n+1}}^h\|\right]^2\}. \end{aligned} \tag{A.16}$$

Thus,

$$\begin{aligned} \frac{1}{2}\|\psi_h^{n+1}\|^2 \geq \frac{1}{4}\left[\|\psi_h^{n+1}\|^2 + ||\phi_h^{n+1}\|^2\right] - \frac{1}{2}\left[\chi\|\eta^{n+1} - \overline{\eta^{n+1}}^h\| + \chi\|u^{n+1} - \overline{u^{n+1}}^h\|\right]\|\phi_h^{n+1}\| \\ + \frac{\chi^2}{4}\left[\|\eta^{n+1} - \overline{\eta^{n+1}}^h\| + \|u^{n+1} - \overline{u^{n+1}}^h\|\right]^2. \end{aligned}$$

Now use (A.15) and (A.16) in the first term in (A.11). This gives

$$\begin{aligned} &\frac{1}{4}\left(\left[\|\psi_h^{n+1}\|^2 + ||\phi_h^{n+1}\|^2\right] - \left[\|\phi_h^{n}\|^2 + \|\psi_h^{n}\|^2\right]\right) + \frac{1}{2}\|\psi_h^{n+1} - \phi_h^n\|^2 + \Delta t\,\frac{\nu}{2}\|\nabla\psi_h^{n+1}\|^2 \\ &\quad + \frac{\chi^2}{4}\left\{\left[\|\eta^{n+1} - \overline{\eta^{n+1}}^h\| + \|u^{n+1} - \overline{u^{n+1}}^h\|\right]^2 - \left[\|\eta^{n} - \overline{\eta^{n}}^h\|^2 + \|u^{n} - \overline{u^{n}}^h\|^2\right]\right\} \\ &\leq C\Delta t\,(1 + \nu^{-3}\|\nabla u^{n+1}\|^4)\|\left(\|\psi_h^{n+1}\|^2 + \|\phi_h^{n+1}\|^2\right) + C\nu\Delta t\|\nabla\eta^{n+1}\|^2 \\ &\quad + C\Delta t\,\|\nabla w_h^{n+1}\|^2\,\|\nabla\eta^{n+1}\|^2 + C\nu^{-1}\Delta t\,\|\nabla u^{n+1}\|^2\|\eta^{n+1}\|\,\|\nabla\eta^{n+1}\| \\ &\quad + C\int_{t^{n-1}}^{t^n}\|\eta_t\|^2\,dt + C\,\Delta t\,\nu^{-1}\|p^{n+1} - q_h\|^2 + \Delta t\,|Intp(u^n;\psi_h^{n+1})| \\ &\quad + \frac{\chi}{2\triangle t}\left[\|\eta^{n+1} - \overline{\eta^{n+1}}^h\| + \|u^{n+1} - \overline{u^{n+1}}^h\|\right]\left[\triangle t\|\phi_h^{n+1}\|\right] \\ &\quad + \frac{\chi}{2\triangle t}\left[\|\eta^{n} - \overline{\eta^{n}}^h\| + \|u^{n} - \overline{u^{n}}^h\|\right]\left[\triangle t\|\psi_h^{n}\|\right]. \end{aligned}$$

The last two terms on the RHS are bounded by

$$\begin{aligned} \text{Next to Last Term: } &\chi\left[\|\eta^{n+1} - \overline{\eta^{n+1}}^h\| + \|u^{n+1} - \overline{u^{n+1}}^h\|\right]\|\phi_h^{n+1}\| \\ &\leq \triangle t\|\phi_h^{n+1}\|^2 + C\triangle t\frac{\chi^2}{\triangle t^2}\left[\|\eta^{n+1} - \overline{\eta^{n+1}}^h\|^2 + \|u^{n+1} - \overline{u^{n+1}}^h\|^2\right], \\ \text{Last Term: } &\frac{\chi}{2\triangle t}\left[\|\eta^{n} - \overline{\eta^{n}}^h\| + \|u^{n} - \overline{u^{n}}^h\|\right]\left[\triangle t\|\psi_h^{n}\|\right] \\ &\leq \triangle t\|\psi_h^{n}\|^2 + C\triangle t\frac{\chi^2}{\triangle t^2}\left[\|\eta^{n} - \overline{\eta^{n}}^h\|^2 + \|u^{n} - \overline{u^{n}}^h\|^2\right]. \end{aligned}$$

Insert these two bounds and sum the result from $n = 1$ to $l - 1$, (noting that $\|\phi_h^0\| = \|\psi_h^0\| = 0$, since $U^0 \in V_h$). We obtain

$$\begin{aligned}
&\frac{1}{4}\left[\|\psi_h^l\|^2 + ||\phi_h^l\|^2\right] + \frac{\chi^2}{4}\left[\|\eta^l - \overline{\eta^l}^h\| + \|u^l - \overline{u^l}^h\|\right]^2 + \sum_{n=1}^{l-1}\frac{1}{2}||\psi_h^{n+1} - \phi_h^n||^2 + \Delta t\sum_{n=1}^{l-1}\frac{\nu}{2}\|\nabla\psi_h^{n+1}\|^2\\
&\le \frac{\chi^2}{4}\left[\|\eta^0 - \overline{\eta^0}^h\|^2 + \|u^0 - \overline{u^0}^h\|^2\right]\\
&+ \Delta t\sum_{n=1}^{l-1} C(1 + \nu^{-3}\|\nabla u^{n+1}\|^4)\left(\|\psi_h^{n+1}\|^2 + \|\phi_h^{n+1}\|^2\right) + C\Delta t\sum_{n=1}^{l-1}\nu\|\nabla\eta^{n+1}\|^2\\
&+ C\Delta t\sum_{n=1}^{l-1}\|\nabla w_h^{n+1}\|^2\,\|\nabla\eta^{n+1}\|^2 + C\nu^{-1}\Delta t\sum_{n=1}^{l-1}\nu^{-1}\|\nabla u^{n+1}\|^2\|\eta^{n+1}\|\,\|\nabla\eta^{n+1}\|\\
&+ C\int_{t_0}^{t_{l-1}}\|\eta_t\|^2\,dt + C\,\Delta t\sum_{n=1}^{l-1}\nu^{-1}\|p^{n+1} - q_h\|^2 + \Delta t\sum_{n=1}^{l-1}|Intp(u^n;\psi_h^{n+1})|\\
&+ \triangle t\sum_{n=1}^{l-1}\|\phi_h^{n+1}\|^2 + C\triangle t\sum_{n=1}^{l-1}\frac{\chi^2}{\triangle t^2}\left[\|\eta^{n+1} - \overline{\eta^{n+1}}^h\|^2 + \|u^{n+1} - \overline{u^{n+1}}^h\|^2\right]\\
&+ \triangle t\sum_{n=1}^{l-1}\|\psi_h^n\|^2 + C\triangle t\sum_{n=1}^{l-1}\frac{\chi^2}{\triangle t^2}\left[\|\eta^n - \overline{\eta^n}^h\|^2 + \|u^n - \overline{u^n}^h\|^2\right].
\end{aligned}$$

Now the last two terms can be collected together to give

$$\begin{aligned}
&\triangle t\sum_{n=1}^{l-1}\|\phi_h^{n+1}\|^2 + C\triangle t\sum_{n=1}^{l-1}\frac{\chi^2}{\triangle t^2}\left[\|\eta^{n+1} - \overline{\eta^{n+1}}^h\|^2 + \|u^{n+1} - \overline{u^{n+1}}^h\|^2\right]\\
&\quad + \triangle t\sum_{n=1}^{l-1}\|\psi_h^n\|^2 + C\triangle t\sum_{n=1}^{l-1}\frac{\chi^2}{\triangle t^2}\left[\|\eta^n - \overline{\eta^n}^h\|^2 + \|u^n - \overline{u^n}^h\|^2\right]\\
&\le \triangle t\sum_{n=1}^{l}\left(\|\phi_h^n\|^2 + \|\psi_h^n\|^2\right) + C\triangle t\sum_{n=1}^{l}\frac{\chi^2}{\triangle t^2}\left[\|\eta^n - \overline{\eta^n}^h\|^2 + \|u^n - \overline{u^n}^h\|^2\right].
\end{aligned}$$

Thus, collecting terms on the RHS, we have

$$\begin{aligned}
&\frac{1}{4}\left[\|\psi_h^l\|^2 + ||\phi_h^l\|^2\right] + \frac{\chi^2}{4}\left[\|\eta^l - \overline{\eta^l}^h\| + \|u^l - \overline{u^l}^h\|\right]^2 \qquad (A.17)\\
&\quad + \sum_{n=1}^{l-1}\frac{1}{2}||\psi_h^{n+1} - \phi_h^n||^2 + \Delta t\sum_{n=1}^{l-1}\frac{\nu}{2}\|\nabla\psi_h^{n+1}\|^2\\
&\le \frac{\chi^2}{4}\left[\|\eta^0 - \overline{\eta^0}^h\|^2 + \|u^0 - \overline{u^0}^h\|^2\right] + \Delta t\sum_{n=1}^{l} C(1 + \nu^{-3}\|\nabla u^n\|^4)\left(\|\psi_h^n\|^2 + \|\phi_h^n\|^2\right)\\
&+ C\Delta t\sum_{n=1}^{l-1}\nu\|\nabla\eta^{n+1}\|^2 + C\Delta t\sum_{n=1}^{l-1}\|\nabla w_h^{n+1}\|^2\,\|\nabla\eta^{n+1}\|^2\\
&+ C\Delta t\sum_{n=1}^{l-1}\nu^{-1}\|\nabla u^{n+1}\|^2\|\eta^{n+1}\|\,\|\nabla\eta^{n+1}\| + C\int_{t_0}^{t_{l-1}}\|\eta_t\|^2\,dt + C\,\Delta t\sum_{n=1}^{l-1}\nu^{-1}\|p^{n+1} - q_h\|^2\\
&+ \Delta t\sum_{n=1}^{l-1}|Intp(u^n;\psi_h^{n+1})| + C\triangle t\sum_{n=1}^{l}\frac{\chi^2}{\triangle t^2}\left[\|\eta^n - \overline{\eta^n}^h\|^2 + \|u^n - \overline{u^n}^h\|^2\right].
\end{aligned}$$

The terms on the RHS of (A.17) are further bounded as follows:

$$C\,\nu\,\Delta t\sum_{n=1}^{l-1}\|\nabla\eta^{n+1}\|^2 \le C\,\nu\,\Delta t\sum_{n=0}^{l}\|\nabla\eta^n\|^2 \le C\,\nu\,\Delta t\sum_{n=0}^{l}h^{2k}|u^n|_{k+1}^2 \le C\,\nu\,h^{2k}|||u|||_{2,k+1}^2. \qquad (A.18)$$

For the next term

$$C\,\nu^{-1}\,\Delta t\sum_{n=1}^{l-1}\|\nabla u^{n+1}\|^2\,\|\eta^{n+1}\|\,\|\nabla\eta^{n+1}\|\ \le\frac{C}{\nu}\,h^{2k+1}\Delta t\sum_{n=1}^{l-1}|u^{n+1}|_{k+1}^2\,\|\nabla u^{n+1}\|^2 \qquad (A.19)$$

$$\le\frac{C}{\nu}\,h^{2k+1}\left(\Delta t\sum_{n=0}^{l}|u^n|_{k+1}^4\,+\,\Delta t\sum_{n=0}^{l}\,\|\nabla u^n\|^4\right)\le\frac{C}{\nu}\,h^{2k+1}\left(|||u|||_{4,k+1}^4\,+\,|||\nabla u|||_{4,0}^4\right)\,.$$

Using the stability bound of $\nu\,\Delta t\,\sum_{n=1}^{l}\|w_h^n\|^2$ by problem data (see Proposition 5.3), we have that

$$C\Delta t\sum_{n=1}^{l}\|w_h^{n+1}\|^2\|\nabla\eta^{n+1}\|^2\le C\nu^{-2}\,h^{2k}\,|||u|||_{\infty,k+1}^2\,. \qquad (A.20)$$

Next

$$C\int_0^{t_l}\|\eta_t\|^2dt\le C\int_0^{t_l}h^{2k+2}\|u_t\|^2\,dt\le C\,h^{2k+2}\,\|u_t\|_{2,k+1}^2, \qquad (A.21)$$

$$\Delta t\sum_{n=1}^{l-1}C\,\nu^{-1}\|p^{n+1}-q_h\|^2\le C\,\nu^{-1}\,\Delta t\sum_{n=1}^{l-1}h^{2s+2}\,\|p^{n+1}\|_{s+1}^2\le C\,\nu^{-1}\,h^{2s+2}\,|||p|||_{2,s+1}^2\,. \qquad (A.22)$$

The consistency error term arising from the backward Euler time discretization in Step 1 is bounded in a standard way. Indeed, adapting the argument in [ELN07], the following *consistency error term* satisfies

$$2\Delta t\sum_{n=1}^{l-1}|Intp(u^n;\psi_h^{n+1})|\le\Delta t\,C\sum_{n=0}^{l}\left(\|\psi_h^n\|^2+\|\phi_h^n\|^2\right)+\epsilon\Delta t\,\nu\sum_{n=1}^{l-1}\|\nabla\psi_h^{n+1}\|^2$$
$$+\,C\Delta t^2\left(\|u_{tt}\|_{2,0}^2\,+\,\|f_t\|_{2,0}^2\,+\,\nu\|\nabla u_t\|_{2,0}^2\right.$$
$$\left.+\,\nu^{-1}\|\nabla u_t\|_{4,0}^4\,+\,\nu^{-1}|||\nabla u|||_{4,0}^4+\nu^{-1}|||\nabla u|||_{4,0}^4\right). \qquad (A.23)$$

Combining (A.18)–(A.23) and collecting terms, equation (A.17) simplifies to

$$\frac{1}{4}\left[\|\psi_h^l\|^2+||\phi_h^l||^2\right]\,+\frac{\chi^2}{4}\left[\|\eta^l-\overline{\eta^l}^h\|\,+\,\|u^l-\overline{u^l}^h\|\right]^2 \qquad (A.24)$$
$$+\sum_{n=1}^{l-1}\frac{1}{2}||\psi_h^{n+1}-\phi_h^n||^2+\Delta t\sum_{n=1}^{l-1}\frac{\nu}{2}\|\nabla\psi_h^{n+1}\|^2$$
$$\le\frac{\chi^2}{4}\left[\,\|\eta^0-\overline{\eta^0}^h\|^2\,+\,\|u^0-\overline{u^0}^h\|^2\right]+\;\Delta t\sum_{n=1}^{l}C(1+\nu^{-3}\|\nabla u^n\|^4)\left(\|\psi_h^n\|^2\,+\,\|\phi_h^n\|^2\right)\,+\,C\,\nu\,h^{2k}|||u|||_{2,k+1}^2$$
$$+\,C\nu^{-2}\,h^{2k}\,|||u|||_{\infty,k+1}^2\,+\,C\,\nu^{-1}\,h^{2k+1}\left(|||u|||_{4,k+1}^4\,+\,|||\nabla u|||_{4,0}^4\right)$$
$$+\,Ch^{2k+2}\,\|u_t\|_{2,k+1}^2+\,C\,\nu^{-1}\,h^{2s+2}\,|||p|||_{2,s+1}^2$$
$$+\,C\Delta t^2\|u_{tt}\|_{2,0}^2+\|f_t\|_{2,0}^2+\nu\|\nabla u_t\|_{2,0}^2+\nu^{-1}\|\nabla u_t\|_{4,0}^4+\nu^{-1}|||\nabla u|||_{4,0}^4+\nu^{-1}|||\nabla u|||_{4,0}^4$$
$$+\,C\triangle t\sum_{n=1}^{l}\frac{\chi^2}{\triangle t^2}\left[\|\eta^n-\overline{\eta^n}^h\|^2\,+\,\|u^n-\overline{u^n}^h\|^2\right].$$

Hence, with Δt sufficiently small, i.e. $\Delta t < C(1 + \nu^{-3}|||\nabla u|||_{\infty,0}^4)^{-1}$, from the discrete Gronwall's Lemma [HeRa], we have

$$\begin{aligned}
&\frac{1}{4}\left[\|\psi_h^l\|^2 + ||\phi_h^l\|^2\right] + \frac{\chi^2}{4}\left[\|\eta^l - \overline{\eta^l}^h\| + \|u^l - \overline{u^l}^h\|\right]^2 \\
&\qquad + \sum_{n=1}^{l-1}\frac{1}{2}||\psi_h^{n+1} - \phi_h^n||^2 + \Delta t\sum_{n=1}^{l-1}\frac{\nu}{2}\|\nabla\psi_h^{n+1}\|^2 \\
&\leq \frac{\chi^2}{4}\left[\|\eta^0 - \overline{\eta^0}^h\|^2 + \|u^0 - \overline{u^0}^h\|^2\right] + C\nu h^{2k}|||u|||_{2,k+1}^2 + C\nu^{-2}h^{2k}|||u|||_{\infty,k+1}^2 \\
&\quad + C\nu^{-1}h^{2k+1}\left(|||u|||_{4,k+1}^4 + |||\nabla u|||_{4,0}^4\right) + Ch^{2k+2}\|u_t\|_{2,k+1}^2 + C\nu^{-1}h^{2s+2}|||p|||_{2,s+1}^2 \\
&\quad + C\Delta t^2\left[\|u_{tt}\|_{2,0}^2 + \|f_t\|_{2,0}^2 + \nu\|\nabla u_t\|_{2,0}^2 + \nu^{-1}\|\nabla u_t\|_{4,0}^4 + \nu^{-1}|||\nabla u|||_{4,0}^4 + \nu^{-1}|||\nabla u|||_{4,0}^4\right] \\
&\quad + C\triangle t\sum_{n=1}^{l}\frac{\chi^2}{\triangle t^2}\left[\|\eta^n - \overline{\eta^n}^h\|^2 + \|u^n - \overline{u^n}^h\|^2\right].
\end{aligned} \tag{A.25}$$

Consider the last term on the above RHS. From Theorem 2.5 and Proposition 5.4 we have (provided $\triangle t < 2$ so $\chi^2/4 < \chi^2/\triangle t^2$)

$$\begin{aligned}
&\frac{\chi^2}{4}\|u^0 - \overline{u^0}^h\|^2 + \triangle t\sum_{n=1}^{l}\left(\frac{\chi}{\triangle t}\right)^2||u^n - \overline{u^n}^h||^2 \\
&\leq C\triangle t\sum_{n=0}^{l}\frac{\chi^2}{\triangle t^2}\inf_{\widetilde{u}^n\in V_h}\left\{\gamma||\nabla\cdot(u^n - \widetilde{u}^n)||^2 + \int_\Omega\delta^2 a(u^n)|\nabla(u^n - \widetilde{u})|^2dx + ||u^n - \widetilde{u}^n||^2\right\} \\
&\qquad + C\delta^4\left(\frac{\chi}{\triangle t}\right)^2\triangle t\sum_{n=0}^{l}||\nabla\cdot(a(u^n)\nabla u^n)||^2 \\
&\leq C\frac{\chi^2}{\triangle t^2}\left[(\gamma+\delta^2)h^{2k+2}\|u\|_{\infty,k+1}^2 + h^{2k+2}\|u\|_{\infty,k+1}^2\right] + C\delta^4\left(\frac{\chi}{\triangle t}\right)^2\triangle t\sum_{n=0}^{l}||\nabla\cdot(a(u^n)\nabla u^n)||^2.
\end{aligned}$$

Thus we have (again provided $\triangle t < 2$ so $\chi^2/4 < \chi^2/\triangle t^2$)

$$\begin{aligned}
&\frac{1}{4}\left[\|\psi_h^l\|^2 + ||\phi_h^l\|^2\right] + \frac{\chi^2}{4}\left[\|\eta^l - \overline{\eta^l}^h\| + \|u^l - \overline{u^l}^h\|\right]^2 \\
&\qquad + \sum_{n=1}^{l-1}\frac{1}{2}||\psi_h^{n+1} - \phi_h^n||^2 + \Delta t\sum_{n=1}^{l-1}\frac{\nu}{2}\|\nabla\psi_h^{n+1}\|^2 \\
&\leq C\nu h^{2k}|||u|||_{2,k+1}^2 + C\nu^{-2}h^{2k}|||u|||_{\infty,k+1}^2 + C\nu^{-1}h^{2k+1}\left(|||u|||_{4,k+1}^4 + |||\nabla u|||_{4,0}^4\right) \\
&\quad + Ch^{2k+2}\|u_t\|_{2,k+1}^2 + C\nu^{-1}h^{2s+2}|||p|||_{2,s+1}^2 \\
&\quad + C\Delta t^2\left\{\|u_{tt}\|_{2,0}^2 + \|f_t\|_{2,0}^2 + \nu\|\nabla u_t\|_{2,0}^2 + \nu^{-1}\|\nabla u_t\|_{4,0}^4 + \nu^{-1}|||\nabla u|||_{4,0}^4 + \nu^{-1}|||\nabla u|||_{4,0}^4\right\} \\
&\quad + C\left(\frac{\chi}{\triangle t}\right)^2\left\{(\gamma+\delta^2)h^{2k+2}\|u\|_{\infty,k+1}^2 + h^{2k+2}\|u\|_{\infty,k+1}^2 + \triangle t\sum_{n=0}^{l}\delta^4||\nabla\cdot(a(u^n)\nabla u^n)||^2\right\} \\
&\quad + C\left(\frac{\chi}{\triangle t}\right)^2\triangle t\sum_{n=0}^{l}\|\eta^n - \overline{\eta^n}^h\|^2.
\end{aligned} \tag{A.26}$$

We now turn to the remaining term involving $\|\eta^n - \overline{\eta^n}^h\|^2$. Recall that $\eta^n = u^n - U^n$. From Proposition 5.4 we have

$$\begin{aligned}
&||\eta^n - \overline{\eta^n}^h||^2 \leq \\
&\leq 4\inf_{\widetilde{v^n}\in V_h}\left\{2\gamma||\nabla\cdot(u^n - \widetilde{v}^n)||^2 + \delta^2||\nabla(u^n - \widetilde{v}^n)||^2 + ||u^n - \widetilde{v}^n||^2\right\} + 4\int_\Omega\delta^2|\nabla(u^n - U^n)|^2dx.
\end{aligned}$$

Thus, by the choice of U^n and $\widetilde{v}^n$, we have

$$\left(\frac{\chi}{\triangle t}\right)^2 \triangle t \sum_{n=0}^{l} \|\eta^n - \overline{\eta^n}^h\|^2 \le 4\left(\frac{\chi}{\triangle t}\right)^2 \triangle t \sum_{n=0}^{l} \int_\Omega \delta^2 |\nabla(u^n - U^n)|^2 dx$$
$$+ C\left(\frac{\chi}{\triangle t}\right)^2 \triangle t \sum_{n=0}^{l} \inf_{\widetilde{v^n}\in V_h} \left\{2\gamma||\nabla\cdot(u^n - \widetilde{v}^n)||^2 + \delta^2||\nabla(u^n - \widetilde{v}^n)||^2 + ||u^n - \widetilde{v}^n||^2\right\}$$
$$\le C\left(\frac{\chi}{\triangle t}\right)^2 \left[\gamma h^{2k}|||u|||^2_{2,k+1} + \delta^2 h^{2k}|||u|||^2_{2,k+1} + h^{2k+2}|||u|||^2_{2,k+1}\right] + C\left(\frac{\chi}{\triangle t}\right)^2 \delta^2 h^{2k}|||u|||^2_{2,k+1}.$$

This gives

$$\frac{1}{4}\left[\|\psi_h^l\|^2 + ||\phi_h^l||^2\right] + \frac{\chi^2}{4}\left[\|\eta^l - \overline{\eta^l}^h\| + \|u^l - \overline{u^l}^h\|\right]^2 \tag{A.27}$$
$$+ \sum_{n=1}^{l-1}\frac{1}{2}||\psi_h^{n+1} - \phi_h^n||^2 + \Delta t\sum_{n=1}^{l-1}\frac{\nu}{2}\|\nabla\psi_h^{n+1}\|^2$$
$$\le C\nu h^{2k}|||u|||^2_{2,k+1} + C\nu^{-2}\,h^{2k}\,|||u|||^2_{\infty,k+1} + C\,\nu^{-1}\,h^{2k+1}\left(|||u|||^4_{4,k+1} + |||\nabla u|||^4_{4,0}\right)$$
$$+ Ch^{2k+2}\,\|u_t\|^2_{2,k+1} + C\nu^{-1}\,h^{2s+2}\,|||p|||^2_{2,s+1}$$
$$+ C\Delta t^2\left[\|u_{tt}\|^2_{2,0} + \|f_t\|^2_{2,0} + \nu\|\nabla u_t\|^2_{2,0} + \nu^{-1}\|\nabla u_t\|^4_{4,0} + \nu^{-1}|||\nabla u|||^4_{4,0} + \nu^{-1}|||\nabla u|||^4_{4,0}\right]$$
$$+ C\left(\frac{\chi}{\triangle t}\right)^2\left[(\gamma + \delta^2)h^{2k+2}\,\|u\|^2_{\infty,k+1} + h^{2k+2}\,\|u\|^2_{\infty,k+1}\right] + C\delta^4\left(\frac{\chi}{\triangle t}\right)^2 \triangle t\sum_{n=0}^{l}||\nabla\cdot(a(u^n)\nabla u^n)||^2$$
$$+ C\left(\frac{\chi}{\triangle t}\right)^2\left[\gamma h^{2k}|||u|||^2_{2,k+1} + \delta^2 h^{2k}|||u|||^2_{2,k+1} + h^{2k+2}|||u|||^2_{2,k+1}\right].$$

The claimed error estimate given then follows from the triangle inequality.

□